

**A NUMERICAL STUDY OF NATURAL CONVECTION
HEAT TRANSFER IN A TRAPEZIFORM CAVITY
FILLED WITH NANOFLUIDS**

by

MD. FAIZAR RAHMAN

Student No. 1015093003P

Session: October 2015


**MASTER OF PHILOSOPHY
IN MATHEMATICS**



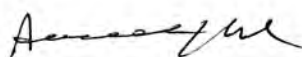
Department of MATHEMATICS
BANGLADESH UNIVERSITY OF ENGINEERING AND TECHNOLOGY, DHAKA
December, 2021

The thesis entitled “A NUMERICAL STUDY OF NATURAL CONVECTION HEAT TRANSFER IN A TRAPEZIFORM CAVITY FILLED WITH NANOFUIDS” submitted by Md. Faizar Rahman, Roll no: 1015093003P, Session: October-2015 has been accepted as satisfactory in partial fulfillment of the requirement for the degree of Master of Philosophy (M.Phil) in Mathematics on 6th December, 2021.


Board of Examiners

- 

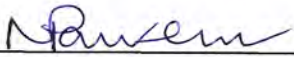
1. **Dr. Rehena Nasrin**
Professor
Department of Mathematics
BUET, Dhaka-1000

Chairman
(Supervisor)
- 

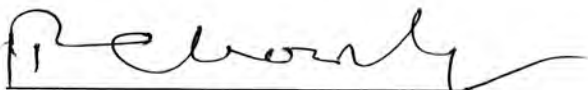
2. **Dr. Md. Abdul Maleque**
Professor
Department of Mathematics
BUET, Dhaka-1000

Member
(Co-Supervisor)
- 

3. **Dr. Khandker Farid Uddin Ahmed**
Professor and Head (Ex-Officio)
Department of Mathematics
BUET, Dhaka-1000

Member
(Ex-officio)
- 

4. **Dr. Nazma Parveen**
Professor
Department of Mathematics
BUET, Dhaka-1000

Member
- 

5. **Dr. Md. Mustafa Kamal Chowdhury**
Former Professor
Department of Mathematics
BUET, Dhaka-1000

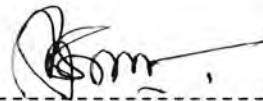
Member
(External)

Certificate of Research

This is to certify that the thesis entitled “**A NUMERICAL STUDY OF NATURAL CONVECTION HEAT TRANSFER IN A TRAPEZIFORM CAVITY FILLED WITH NANOFUIDS**” that Md. Faizar Rahman is submitting in partial fulfillment for the award of M.Phil. The author has carried out-degree in MATHEMATICS under the supervision of Dr. Rehana Nasrin, Professor, Department of Mathematics, Bangladesh University of Engineering and Technology, Dhaka-1000. The fore-fold outcome embodied in this thesis has not been produced either by any other university or institute for the award of any degree or diploma.



Dr. Rehana Nasrin
Professor
Department of Mathematics
BUET, Dhaka-1000



Md. Faizar Rahman
Students ID: 1015093003P
Session: October, 2015

Candidate's Declaration

It is out of my best to ensure the thesis entitled “**A NUMERICAL STUDY OF NATURAL CONVECTION HEAT TRANSFER IN A TRAPEZIFORM CAVITY FILLED WITH NANOFLUIDS**” I have prepared it with the guidance of **Dr. Rehana Nasrin**, Professor, Department of Mathematics, BUET as supervisor and **Dr. Md. Abdul Maleque**, Former Professor, Department of Mathematics, Bangladesh, BUET as co-supervisor. As a result, I declare that the results presented in this thesis are original and have not been submitted, in part or whole, for any degree, diploma, fellowship, etc., of any other University or Institution. Furthermore, I have duly acknowledged all the sources of information that have been used in the thesis.



Md. Faizar Rahman
Students ID: 1015093003
Session: October, 2015

**This work is dedicated to
My Son and Daughter**

Acknowledgement

I would like to affirm the continual mercy, help, and blessing showered by the Almighty without which it would have been impossible to accomplish the arduous job I was assigned to.

With great pleasure, I would like to express my deep and sincere gratitude to my respected supervisor **Dr. Rehena Nasrin**, Professor, Department of Mathematics, Bangladesh University of Engineering and Technology, and co-supervisor **Dr. Md. Abdul Maleque**, Former Professor, Department of Mathematics, Bangladesh University of Engineering and Technology (BUET), Dhaka-1000 for their expert guidance and valuable suggestions throughout this work. Their priceless suggestions make this work interesting and learning to me. It would not have been possible to carry out this study successfully without the continuous inspiration and encouragement from my supervisor and co-supervisor.

I owe a favor to **Dr. Khandker Farid Uddin Ahmed**, Professor, and Head, Department of Mathematics, BUET, for his support in allowing me to use the departmental facilities in various stages of my work. I also thank all the staff of the Department of Mathematics, BUET for being so helpful.

I would like to offer my humble gratitude and profound respect to **Dr. Nazma Parveen**, Professor, Department of Mathematics, BUET for her comments and constructive concept which helped me to better understand the issues of this thesis.

I am indebted to the external member of the Board of Examiners, **Dr. Md. Mustafa Kamal Chowdhury**, Former Professor, Department of Mathematics, BUET, Dhaka-1000.

Finally, I would like to express my gratitude to my dear wife, son, and daughter for their steadfast love and support. They have kept me going through the most difficult times.

Abstract

The present research has intended numerically the steady of laminar natural convective flow and heat transfer in a trapeziform cavity filled with nanofluid. The heat transferring medium has been taken as water-ferrosopherric oxide (Fe_3O_4) and water-copper (Cu) nanofluids. The trapeziform cavity has been accurately propounded by uniformly heated bottom wall with two types of temperature distributions like constant temperature and sinusoidal temperature, constant temperature of cold top wall, adiabatic other two walls and no-slip condition of all walls. The governing partial differential equations for nanofluid have been transformed into the non-dimensional form using similarity transformation, then modified into finite element equations and finally solved. The influence of various values of the buoyancy parameter, Rayleigh number ($10^3 \leq Ra \leq 10^6$), Prandtl number ($0.7 \leq Pr \leq 5.8$) and nanoparticle volumetric ratio ($0 \leq \phi \leq 0.03$) has been investigated numerically and described the results in this thesis. The results have been addressed and visually represented using streamlines and isothermal lines for velocity and temperature contours, as well as average Nusselt number for heat transfer rate. The Rayleigh number, Prandtl number and nanosolid volumetric ratio all have a substantial influence on the convective flow regime, and the value of average Nusselt number changes as these parameters change. Due to the greater value of the Rayleigh number ($Ra = 10^6$), the average Nusselt number increases to 18.6% for sinusoidal temperature and 21.6% for constant temperature distribution at the hot bottom wall of the trapeziform enclosure using water- Fe_3O_4 nanofluid. The water- Fe_3O_4 nanofluid achieves a greater rate of heat transfer (5.83% for sinusoidal temperature and 7.38% for constant temperature distribution) than the base fluid (water). The solid volume fraction increases 0% to 3%, the mean Nusselt number increases 12.67% for sinusoidal temperature and 15.57% for constant temperature distribution using water-Cu nanofluid at the hot bottom wall of the trapeziform enclosure. Compared to water- Fe_3O_4 nanofluid, the Cu-water nanofluid achieves a greater rate of heat transfer 6.77% for sinusoidal temperature and 7.63% for constant temperature distribution at bottom wall using solid volume fraction $\phi = 0.03$.

Contents

Abstract.....	vii
List of Tables	xi
List of Figures.....	xii
Chapter 1: Introduction	1
1.1 Introduction	1
1.2 Keywords definition and description	2
1.2.1 Heat transfer.....	2
1.2.2 Nanoparticles	2
1.2.3 Nanofluids	3
1.2.4 Convection heat transfer	5
1.2.5 Natural convection heat transfer	5
1.2.6 Viscosity	6
1.2.7 Thermal conductivity.....	7
1.2.8 Thermal diffusivity.....	7
1.2.9 Nanoparticles solid volume fraction	8
1.3 Dimensionless Parameter	8
1.3.1 Rayleigh number	9
1.3.2 Prandtl number	9
1.3.3 Nusselt number.....	10
1.4 Literature Review.....	10
1.5 Objectives.....	13
1.6 Possible Outcomes	13
1.7 Scope of the Thesis	14
Chapter 2: Numerical Analysis.....	15
2.1 Introduction.....	15

2.2	Finite Element Method	15
2.3	Problem Formulation	16
2.3.1	Physical model	16
2.3.2	Mathematical modeling	17
2.3.3	Thermo-physical properties	19
2.4	Numerical Analysis.....	20
2.4.1	Grid sensitivity test	20
2.4.2	Meshing.....	22
2.4.3	Validation of the numerical scheme	23
	Chapter 3: Results and Discussions.....	25
3.1	Introduction	25
3.2	Effect of Rayleigh Number	25
3.3	Effect of Prandtl Number	29
3.4	Effect of Solid Volume Fraction.....	32
3.5	Nusselt Number	35
3.6	Comparison.....	37
3.6.1	Comparison with Basak <i>et al.</i> [51]	37
3.6.2	Comparison with Weheibi <i>et al.</i> [51]	38
	Chapter 4: Conclusions and Future Research	40
4.1	Conclusions	40
4.2	Future Research.....	41
	References	42

Nomenclature

C_p	Specific heat at constant pressure ($\text{Jkg}^{-1}\text{K}^{-1}$)
g	Gravitational force (ms^{-2})
k	Thermal conductivity ($\text{Wm}^{-1}\text{K}^{-1}$)
Nu	Nusselt number
p	Pressure (kgms^{-2})
Pr	Prandtl number
n	Dimensional distance
N	Non-dimensional distance
Ra	Rayleigh number
T	Dimensional temperature (K)
u, v	Dimensional x and y components of velocity (ms^{-1})
U, V	Dimensionless velocities
x, y	Cartesian coordinates (m)

Greek Symbols

α	Thermal diffusivity (m^2/s)
β	Coefficient of thermal expansion ($1/\text{K}$)
θ	Dimensionless temperature
μ	Dynamic viscosity (Nsm^{-2})
ρ	Density (kgm^{-3})
φ	Volume fraction (%)

Subscripts

c	Cold
f	Fluid (water)
h	Hot
nf	Nanofluid
s	Solid particle

Abbreviation

FEA	Finite element analysis
FEM	Finite element method
HTF	Heat transferring fluid

List of Tables

Items	Table Caption	Page
Table 1.1	Thermal conductivity of some materials, base fluids, and nanofluids	8
Table 2.1	Thermo-physical properties of the base fluids and the solid nanoparticles	20
Table 2.2	The average Nusselt number for the various number of grid elements at $Ra = 10000$, $Pr = 5.8$, $\phi = 0.01$ and constant temperature of bottom surface	21
Table 3.1	Comparison of average Nusselt number between present numerical study and the research of Basak <i>et al.</i> [51] in terms of Rayleigh number	38
Table 3.2	Comparison of average Nusselt number between present numerical study and the research of Weheibi <i>et al.</i> [52] in terms of Rayleigh number	39

List of Figures

Items	Figure Caption	Page
Figure 1.1	Heat transfer system	2
Figure 1.2	Nanoparticles	3
Figure 1.3	Nanofluids mechanism	4
Figure 1.4	Different types of nanofluid	4
Figure 1.5	Convection Heat Transfer	5
Figure 1.6	Natural Convection Heat Transfer	6
Figure 1.7	Viscosity of fluid	7
Figure 2.1	Physical model	17
Figure 2.2	The average Nusselt number (Nu) for various number of elements	21
Figure 2.3	The processing time in second for various number of elements	22
Figure 2.4	FEM Mesh	23
Figure 2.5	Code validation of present result	24
Figure 3.1	The streamlines for Rayleigh number variation with (a) constant temperature and (b) sinusoidal temperature at bottom wall	27
Figure 3.2	The isothermal lines for Rayleigh number variation with (a) constant temperature and (b) sinusoidal temperature at bottom wall	28
Figure 3.3	The streamlines for Prandtl number variation with (a) constant temperature and (b) sinusoidal temperature at bottom wall	30
Figure 3.4	The isothermal lines for Prandtl number variation with (a) constant temperature and (b) sinusoidal temperature at bottom wall	31
Figure 3.5	The streamlines for solid volume fraction variation with (a) constant temperature and (b) sinusoidal temperature at bottom wall	33
Figure 3.6	The isothermal lines for solid volume fraction variation with (a) constant temperature and (b) sinusoidal temperature at bottom wall	34
Figure 3.7	The average Nusselt number for Rayleigh numbers variation	35
Figure 3.8	The average Nusselt number for Prandtl numbers variation	36
Figure 3.9	The average Nusselt number for solid volume fraction variation	36
Figure 3.10	Comparison of average Nusselt number between Basak <i>et al.</i> [51] and present research	37
Figure 3.11	Comparison of average Nu between Webeibi <i>et al.</i> [52] and present research	38

1.1 Introduction

Fluid Mechanics is a significant branch of applied mechanics that studies the behavior of fluids (liquids and gases) at rest and in motion and their interactions with their surroundings. The most misunderstood thermodynamic principles are heat and temperature. Theoretically, the principles of heat and temperature are discussed together in physics, but they are not similar. In another way, heat is the flow of energy from one substance to another due to a temperature differential, and it can change the state of temperature. Furthermore, temperature is a physical condition that is determined by an object's molecular activity.

The branch of applied thermodynamics that deals with the transfer of heat are called heat transfer. It calculates the rate at which heat is transmitted through system borders, taking into account absolute temperature variations and the system's temperature distribution during the operation. On the other hand, classical thermodynamics is concerned with the amount of heat exchanged during the process. Since the thermal conductivity of these fluids plays a significant role in the heat transfer coefficient between the heat transfer medium and the heat transfer surface, several experiments over the last decade have concentrated on modelling thermal conductivity and analyzing various viscosities of nanofluid. As a result, various theoretical and experimental experiments have been performed to boost the thermal conductivity of fluids by suspending nano/micro-sized particles/materials in insufficient heat transfer fluids such as tar, water, and ethylene glycol mixture.

Natural, buoyant, or free convection is an important phenomenon that occurs in various natural environments. The motion of density gradients in conjunction with a gravitational field causes it. It is used in multiple uses, including building energy storage, electrical device cooling, nuclear reactor cooling, solar engineering, environmental and geothermal fluid dynamics. Electronic system cooling, double-pane walls, house heating and cooling, refrigerators, space ventilation, heat exchangers, solar collectors, and other applications are among them.

Nanofluid is a modern heat transfer medium that includes nanoparticles (1–100 nm) dispersed uniformly and continuously in a base fluid. The thermal conductivity of the nanofluid is significantly improved by these scattered nanoparticles, which are typically metal or metal oxide. These are enhanced conduction and convection coefficients, allowing

for more heat transfer. Using nanofluid in heat transfer improvement for improving the performance of thermal systems such as heat exchangers, thermal storage, solar collectors, photovoltaic/thermal systems, biomedical equipment, nuclear reactors, cooling of electronic parts, and so on is one of the practical passive approaches. Therefore, in the present study, attention will be focused on the effect of free convection heat transfer of nanofluid presence in a trapeziform enclose and the obtained numerical results is validated by comparing them with those obtained from numerical software.

1.2 Keywords

There are a few keywords related to this research. The definitions and descriptions of them have been given below:

1.2.1 Heat transfer

Heat transfer describes the exchange of thermal energy, between physical systems depending on the temperature and pressure, by dissipating heat. Figure 1.1 expresses general heat transfer procedure. The fundamental modes of heat transfer are conduction or diffusion, convection (free and forced) and radiation. Thermal equilibrium is reached when all involved bodies and the surroundings reach the same temperature.

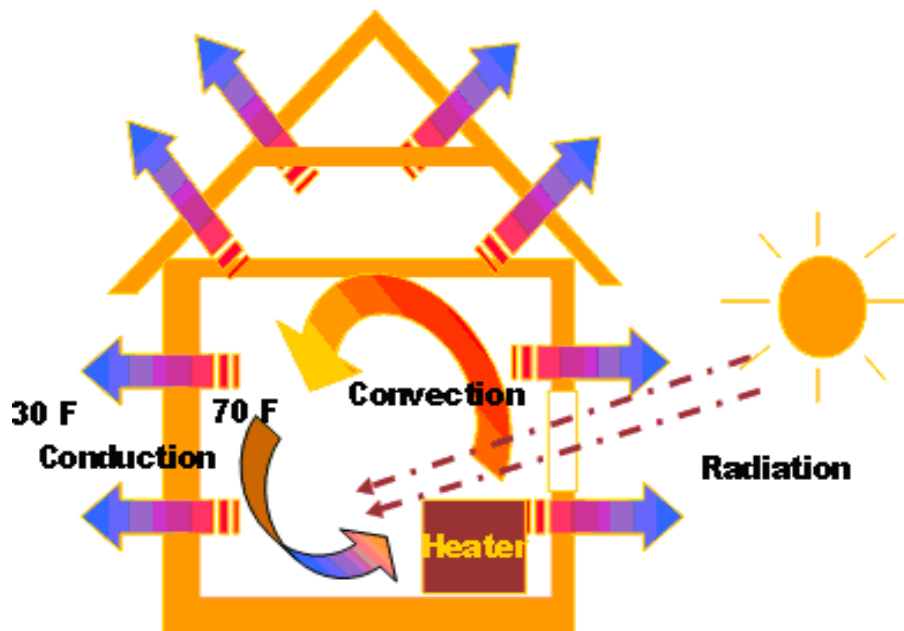


Figure 1.1: Heat transfer system

1.2.2 Nanoparticles

A nanoparticle is a tiny molecule with a diameter of 1 to 100 nanometers. Nanoparticles, invisible to the naked eye, may have substantially different physical and chemical properties

than their larger substance equivalents. According to the European Commission's concept, at least half of the particles in a number size distribution must have a particle size of 100 nm or less. The bulk of nanoparticles comprise just a few hundred atoms. Copper, for example, is called a soft substance when the atoms swarm at the 50nm range, causing bulk copper to bend. As a result, copper nanoparticles smaller than 50nm are deemed a tough substance, with much lower malleability and ductility than bulk copper. In addition, their size often influences the melting properties of gold nanoparticles; gold nanoparticles melt at far lower temperatures (300°C for 2.5 nm size) than bulk gold (1064°C). Furthermore, solar radiation absorption is significantly stronger in nanoparticle-based materials than in thin films of flat sheets of glass.

Nanoparticles which are commonly used in nanofluids are made from numerous materials such as oxide ceramics (Al_2O_3 , CuO), nitride ceramics (AlN , Si_3N_4), carbide ceramics (SiC , TiC), metals (Cu , Ag , Au), semiconductors (TiO_2 , SiC), carbon nanotubes, and composite materials such as alloyed nanoparticles, $\text{Al}_{70}\text{Cu}_{30}$ or nanoparticle core-polymer shell composites. Image 1.2 is showing nanoparticles of an alloy of gold (yellow) and palladium (blue) on acid-treated carbon support (gray). These particles were employed as catalysts to form hydrogen peroxide from hydrogen (white) and oxygen (red).

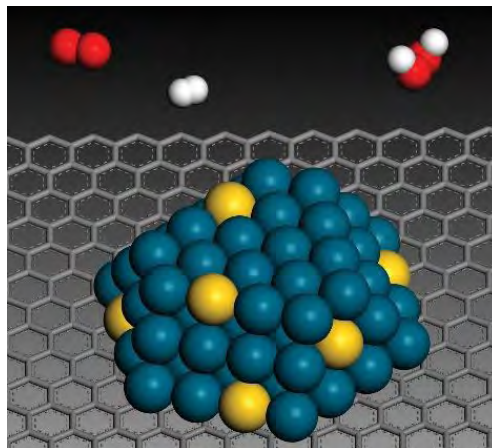


Figure 1.2: Nanoparticles

1.2.3 Nanofluids

The fluid in which solid-sized nanoparticles are suspended is known as "nanofluid." Nanofluid, in other words, is a fluid containing nanometer-sized (1-10 nm) particles known as nanoparticles. Choi [52] of the Argonne National Laboratory in the United States invented the word "nanofluids" in 1995 (diameter less than 50nm). Metals, oxides, carbides, and

carbon nanotubes are commonly used as nanoparticles in nanofluids. Common base fluids include water (H₂O), ethylene glycol (EG), engine oil (EO), pump oil, and glycerol have been used as host liquids in nanofluids. Figure 1.3 shows the mechanism of nanofluids. Many types of nanoparticles such as metals (Cu, Ag, Au), oxide ceramics (Al₂O₃, CuO), carbon nanotubes, and carbide ceramics (SiC, TiC), and various liquids such as water, oil, and ethylene glycol are used.

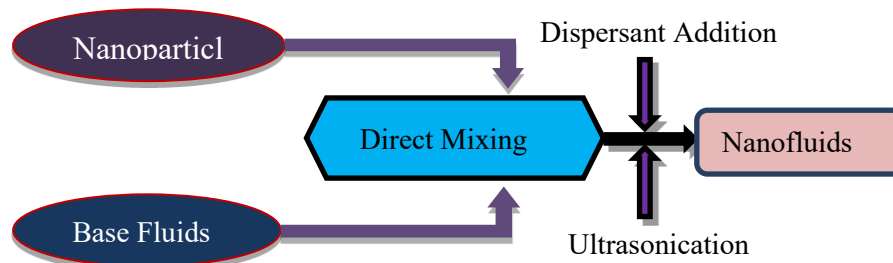


Figure 1.3: Nanofluids

For example, figure 1.4 shows different types of nanofluid. The aim of creating nanofluids is to use them as thermo-fluids in heat exchangers to increase heat transfer coefficient and, as a result, reduce the size of heat transfer equipment. Nanofluids assist in heat energy and heat exchanger content storage. Thermal conductivity, viscosity, natural heat, and density are significant parameters that affect the heat transfer characteristics of nanofluids.

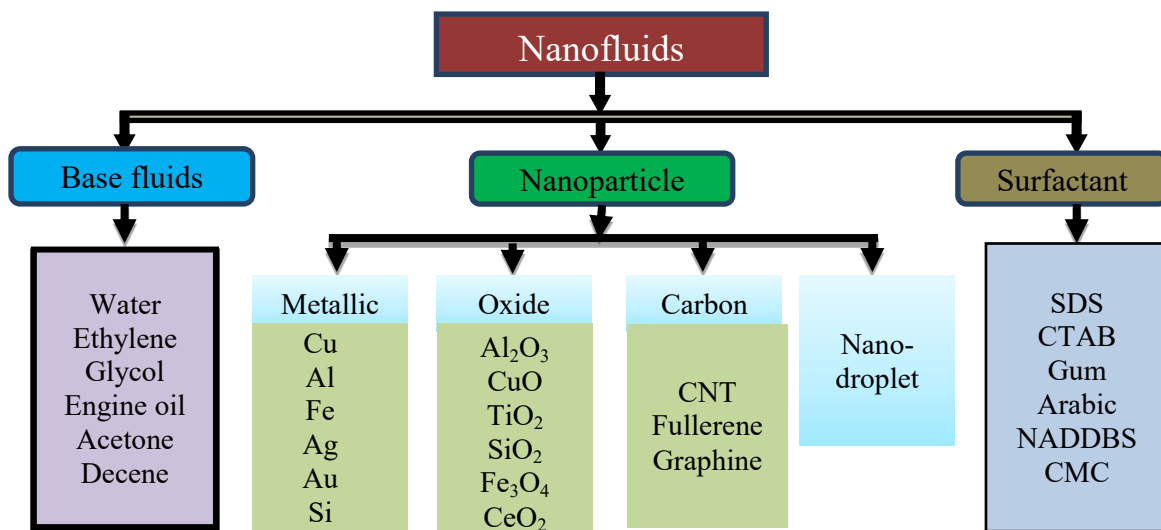


Figure 1.4: Different types of nanofluid

Their working temperature often influences nanofluids' thermo-physical properties. As a result, precise temperature-dependent property measurements of nanofluids are essential. Nanofluid thermo-physical properties are needed for calculating the heat transfer coefficient and the Nusselt number. Some typical applications are: -

- Engine cooling and transmission oil
- Boiler exhaust flue gas recovery
- Cooling of electronic circuits
- Nuclear system cooling
- Solar water heating
- Refrigeration (domestic and chillers)
- Defense and Space applications
- Thermal storage
- Bio-medical applications
- Drilling and lubrications

1.2.4 Convective heat transfer

Transfer of heat from one place to another due to the molecular movement of fluids (Air or liquids) is known as convection heat transfer. When molecules move from one place to another they carry heat with them. Convective heat transfer can be classified into two types, natural convection and forced convection. Here we have discussed about natural convection heat transfer. The geometry has been shown for convective heat transfer in the figure 1.5.

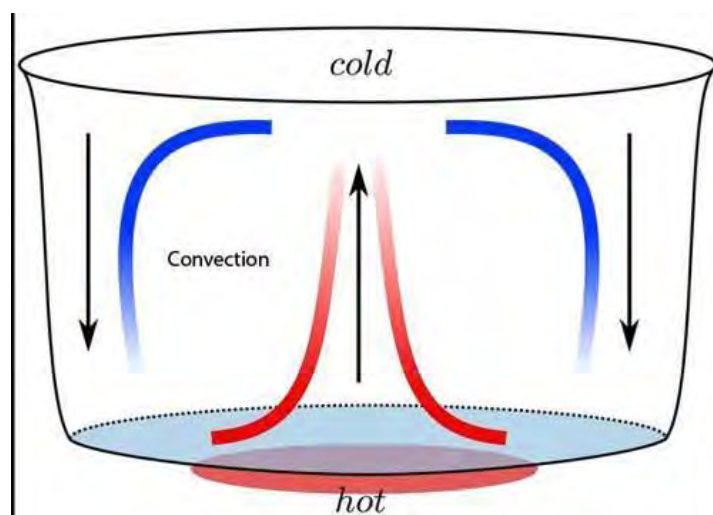


Figure 1.5: Convective heat transfer

1.2.5 Natural convective heat transfer

Natural convection is a type of flow, of motion of a liquid such as water or a gas such as air, in which the fluid motion is not generated by any external source (like a pump, fan, suction device, etc.) but by some parts of the fluid being heavier than other parts. The driving force for natural convection is gravity. For example, if there is a layer of cold dense air on top

of hotter less dense air, gravity pulls more strongly on the denser layer on top, so it falls while the hotter less dense air rises to take its place. This creates circulating flow: convection. As it relies on gravity, there are no convection in free-fall (inertial) environments, such as that of the orbiting International Space Station. Natural convection can occur when there are hot and cold regions of either air or water because both water and air become less dense as they are heated. But, for example, in the world's oceans, it also occurs due to salt water being heavier than freshwater, so a layer of salt water on top of a layer of fresher water will also cause convection. Natural convection has attracted a great deal of attention from researchers because of its presence both in nature and engineering applications. In nature, convection cells formed from air raising above sunlight-warmed land or water are a major feature of all-weather systems (figure 1.6).

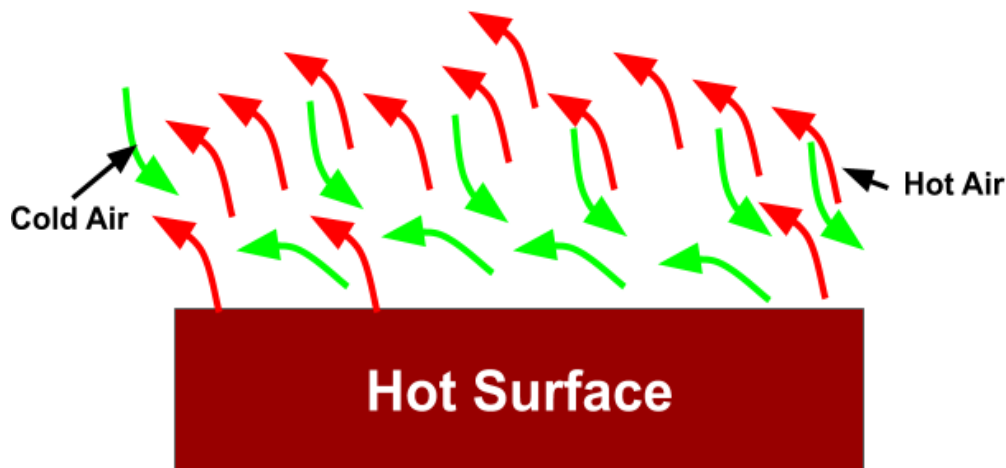


Figure 1.6: Natural convective heat transfer

1.2.6 Viscosity

A fluid's viscosity measures its resistance to progressive deformation caused by shear or tensile stress. It refers to the informal definition of "thickness" of liquids: syrup, for example, has a higher viscosity than wine. The frictional force between two neighboring layers of fluid in relative motion may be thought of as viscosity. For example, when a fluid is squeezed into a funnel, the fluid travels faster along the tube's axis and slower along the tube's walls. Experiments demonstrate that some friction (such as a pressure differential between the tube's two ends) is needed to keep the flow moving through the line. This is because a force is required to counteract friction between the fluid layers in relative motion, and the intensity of this force is proportional to the viscosity. The term "ideal" or "inviscid" refers to a fluid with no tolerance to shear tension. In super fluids, zero viscosity is only found at shallow temperatures. Otherwise, the second rule of thermodynamics specifies that all fluids have positive viscosity; those fluids are called viscous or viscid in scientific terms. Pitch, for

example, has an extreme viscosity and can look rigid. Figure 1.7 depicts fluids of high and low viscosity.

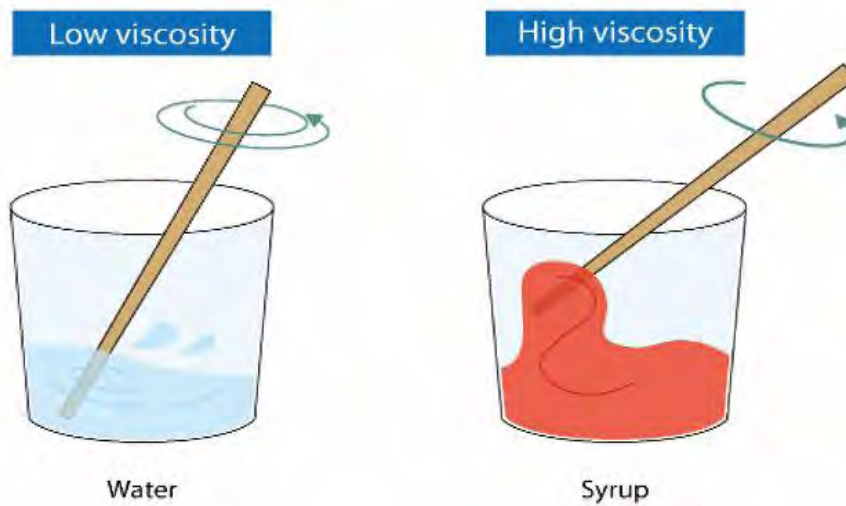


Figure 1.7: Viscosity of fluid

1.2.7 Thermal conductivity

The volume and intensity at which heat is transferred through a substance are referred to as thermal conductivity. Heat transfer is faster in high thermal conductivity materials than in low thermal conductivity materials. High thermal conductivity materials are commonly used in heat sink applications, whereas low thermal conductivity materials are used in thermal insulation. The thermal conductivity of materials varies with temperature. Thermal resistivity is the reciprocal of thermal conductivity. Copper, for example, has high electrical conductivity and has poor thermal conductivity. The heat produced in high thermal conductivity materials is quickly transferred away from the weld region. Electrical and thermal conductivity are strongly correlated in metallic products; materials with high electrical conductivity (low electrical resistance) often have high thermal conductivity. The proportionality constant k describes the material's thermal conductivity. The thermal conductivity k is calculated as follows:

$$k = \frac{\text{Heat flow } (Q) \times \text{Thickness of the material } (L)}{\text{Surface area of material } (A) \times \text{Temperature gradient } (\Delta T)}$$

1.2.8 Thermal diffusivity

Thermal diffusivity is the rate at which heat is transferred from one side of a substance to the other. At constant pressure, it can be determined by dividing thermal conductivity by density and specific heat power. Thermal diffusivity is characterized as the rate at which heat diffuses through a

substance, and it defines as $\alpha = \frac{k}{\rho c_p}$

Here k is thermal conductivity $\left[\frac{W}{(m \cdot K)}\right]$, ρ is density $\left[\frac{kg}{m}\right]$, and c_p is the specific heat capacity

$\left[\frac{J}{(kg \cdot K)} \right]$. A substance with a robust thermal diffusivity would have a high thermal conductivity or a low heat capacity. The more the heat propagates through the medium, the higher the thermal diffusivity. A low thermal diffusivity value indicates that the substance consumes much heat, and only a limited amount is performed further.

1.2.9 Nanoparticles solid volume fraction

The volume fraction φ is determined by dividing the volume of nanoparticles by the total volume of the nanofluid's constituents. In optimal solutions, where the volumes of the components are proportional, the volume fraction corresponds to the volume concentration (the volume of the solution is equal to the sum of the volumes of its ingredients). According to Yang *et al.* [6], the volumetric fraction of nanoparticles, shape, and size of nanomaterials all influence the properties of nanofluids. For example, Table 1.1 illustrates how suspending particles increase the thermal conductivity of nanofluid in contrast to the base fluid.

Table 1.1: Thermal conductivity of some materials, base fluids, and nanofluids

	Materials	Thermal conductivity (W/mk)
Metallic Materials	Copper	401
	Silver	429
	Iron	84
Nonmetallic Materials	Silicon	148
	Alumina (Al ₂ O ₃)	40
Carbon	Carbon Nano Tubes (CNT)	2000
Base fluids	Water	0.613
	Ethylene glycol (EG)	0.253
	Engine oil (EO)	0.145
Nanofluids (Nanoparticle concentration, %)	Water/ Al ₂ O ₃ (1.50)	0.629
	EG/ Al ₂ O ₃ (3.00)	0.278
	EG-Water/ Al ₂ O ₃ (3.00)	0.382
	Water/ TiO ₂ (0.75)	0.682
	Water/ CuO (1.00)	0.619

1.3 Dimensionless Parameters

In fluid dynamics, dimensionless parameters are a collection of dimensionless quantities that play an important role in fluid behavior. Mechanical engineers often deal with numbers that have no dimensions. They are either pure quantities with no units or groupings of variables

under which the units cancel each other precisely, resulting in a pure number. For example, a dimensionless integer can be the ratio of two other quantities, in which case the numerator and denominator dimensions cancel out. The dimensionless parameters may be thought of as weighted averages of the relative value of different dimensions of the flow. The following are several dimensionless parameters relevant to the current study:

1.3.1 Rayleigh number

In fluid mechanics, the Rayleigh number (Ra) for a fluid is a dimensionless number associated with buoyancy-driven flow, also known as free or natural convection. The Rayleigh number describes the behavior of fluids (such as water or air) when the mass density of the fluid is non-uniform. The mass density differences are usually caused by temperature differences. Typically, a fluid expands and becomes less dense as it is heated. Gravity causes denser parts of the fluid to sink, which is called convection. Lord Rayleigh studied the case of Rayleigh- Bénard convection. When the Rayleigh number, Ra , is below a critical value for a fluid, there is no flow, and heat transfer is purely by conduction; when it exceeds that value, heat is transferred by natural convection. When the mass density difference is caused by the temperature difference, Ra is, by definition, the ratio of the time scale for diffusive thermal transport to the time scale for convective thermal transport at speed u .

$$Ra = \frac{\text{time scale for thermal transport via diffusion}}{\text{time scale for thermal transport via convection of speed } u}$$

Thus, the Rayleigh number is $= \frac{g\beta(T_h - T_c)H^3}{\alpha\nu}$, where β = Thermal coefficient, $T_h - T_c$ = Temperature difference, g = Constant of gravity, ν = Kinematic viscosity and α = Thermal diffusivity. The Rayleigh number can be written as the product of the Grashof number and the Prandtl number, i.e. $Ra = GrPr$.

1.3.2 Prandtl number

The relative thickness of the velocity and the thermal boundary layers are best described by the dimensionless parameter Prandtl number. Prandtl number is a dimensionless number, named after the German physicist Ludwig Prandtl, defined as the ratio of kinematic viscosity to thermal diffusivity and may be written as follows

$$Pr = \frac{\text{Kinematic viscosity}}{\text{Thermal diffusivity}} = \frac{\nu}{\alpha}$$

The value of ν shows the effect of viscosity of the fluid. The smaller the value of ν is the

narrower of the region which is affected by viscosity and which is known as the boundary layer region when ν is very small. The value of α shows the thermal diffusivity due to heat conduction. The smaller the value of α is the narrower of the region which is affected by the heat conduction, and which is known as thermal boundary layer when D_T is small. Thus, the Prandtl number shows the relative importance of heat conduction and viscosity of a fluid.

1.3.3 Richardson number

The Richardson number can be used to predict the occurrence of fluid turbulence and, hence, the destruction of density currents in water or air. It was defined by the British meteorologist Lewis Fry Richardson, a pioneer in mathematical weather forecasting. Essentially the ratio of the density gradient (the change in density with depth) to the velocity gradient, the Richardson number is defined as

$$Ri = \frac{g}{\rho} \frac{\partial \rho}{\partial z} / \left(\frac{\partial u}{\partial z} \right)^2$$

in which g is gravity, ρ is density, u is velocity, and z is depth.

1.3.4 Nusselt number

The Nusselt number is the ratio of convective to conductive heat transfer across a boundary. The convection and conduction heat flows are parallel to each other and to the surface normal of the boundary surface, and are all perpendicular to the mean fluid flow in the simple case.

$$Nu = \frac{\text{Convective heat transfer}}{\text{Conductive heat transfer}} = \frac{h}{k/L} = \frac{hL}{k}$$

1.4 Literature Review

M. Hasnaoui *et al.* [1] a two-dimensional numerical study of natural convection heat transfer in a rectangular enclosed cavity with localized heating from below has been carried out. Arici and Sahin [2] numerically investigated the natural convection in a partially divided trapezoidal enclosure by using the control volume method. The steady free convection of air-flow in a 2-D side-heated trapezoidal room has been numerically investigated by Lasfer *et al* [3]. The geometry considered was, a vertical right cooled sidewall, an inclined left heated sidewall, and two isolated horizontal lower and upper walls. The obtained results showed a great dependence of the heat transfer on inclination angle, the flow fields, Rayleigh number and aspect ratio.

Recently, Selimefendigil *et al.* [4] numerically studied the mixed convection in a lid-driven

3-D flexible walled trapezoidal enclosure with nanofluids using finite element method based on Galerkin weighted residuals. They concluded that the fluid flow and heat transfer characteristics are influenced by the variations in the elastic modulus of the side wall, Richardson number and volume fraction of nanoparticle for different side wall inclination angles of the trapezoidal cavity. Extensive investigations have also been carried out to study the heat transfer convection in the fluid-saturated porous medium because of its applicability in various industrial applications concerning the geothermal fields [5], process of phase change [6], applications of heat exchanger [7], bio-engineering [8], *etc.* Recently, various studies on free and mixed convection in the porous cavities with many geometrical shapes were carried out by many researchers [9-16]. The trapezoidal enclosures are useful in many applications and many studies were presented in the literature based on the practical applications.

Free convective in the trapezoidal cavities (both fluid and porousmedia) are highly useful for applications in desalination [17], the green house type solar stills [18], solar cavity receiver [19], *etc.* Although various attempts were made to study the natural convection in irregular porous cavities, the study of effects of heat generation and porosity on natural convection in the porous trapezoidal cavities with linearly heated inclined wall (s) is yet to appear in the literature. Appropriate modeling of convective heat transport can be ensured the utility of a particular nanofluid. Several scientists' have undertaken diverse studies discussing the convection process in the nanofluid filled trapezoidal cavity. Mahmoodi [20] conducted a comprehensive overview of recent nanofluid studies that would be useful to researchers working on the topic. Many experimental and theoretical experiments have been carried out (both numerical and analytical). Due to its ability in heat transfer enhancement applications, nanofluid has been the subject of intensive research over the last decade.

Soleimani *et al.* [21] studied natural convection heat transfer within a copper-water nanofluid filled a semi-annulus cavity. Their results showed that there is an optimum angle of turn for which the rate of heat transfer is maximum for several thermal Rayleigh numbers. Roslan *et al.* [22] investigated the buoyancy-driven heat transfer within a nanofluid filled trapezoidal cavity with variable thermal conductivity and viscosity. They reported that the effect of the viscosity was more dominant than the thermal conductivity in heat transfer augmentation and heat transfer enhancement is not that much noticeable for using nanofluid.

Nanofluids have considerable potential in microelectronics, medicinal systems, fuel cells, hybrid motors, refrigerators, chillers, and heat exchangers, among other applications. The

insights of nanofluids, hybrid nanofluids flow, and applicability of nanofluids can be seen in articles [23-25]. Aghaei *et al.* [26] studied the effects of magnetic field and entropy generation on mixed convection utilizing nanofluid in a trapezoidal enclosure. They found that the magnetic field shrinks the convective heat transfer and flow strength of nanofluid. The insignificant measurement of entropy generation notices for frictions whereas noteworthy entropy generation takes place for an irreversible state of heat transfer. Alipour *et al.* [27] studied the influence of T-semi attached rib on turbulent flow and heat transfer parameters of a silver-water nanofluid with different volume fractions in a three-dimensional trapezoidal microchannel. They showed that the heat transfer coefficient is increased as the Reynolds number and volume fraction of solid nanoparticle are increased.

The performance of the heat transfer of nanofluids depends on some crucial parameters such as nanofluids' size, shape, constructive materials of base fluids, concentration, etc. [28-31]. It is reported that nanofluids are used as a momentum to enhance the heat transfer. For engineering research, free convection or natural convection in cavities of various geometries plays an important role. It has a broad range of technical uses, including solar applications, construction applications, and the electrical industry. In a very recent time, many researchers are getting interested in working on nanofluids because of the increasing demand of the uses of nanofluids in a different area and also, they have focused on the heat transfer properties of nanofluids of different shapes, namely, square shaped by Roy [32] and Al-Balushi *et al.* [33], triangular shaped by Mancour *et al.* [34] and Arani *et al.* [35], rectangular shaped by Bouhaleb *et al.* [36], triangular wavy shaped by Nasrin *et al.* [37], C-shaped by Makulati *et al.* [38], semi annulus shaped by Soleimani *et al.* [39], and annulus shaped by Roy [40].

Selimefendigil *et al.* [41] numerically investigate an inner rotating cylinder with a flexible wall and square cavity filled with SiO₂-water nanofluids. It has shown that, among the all-nanoparticles, cylindrical shape nanoparticles provide the best output, and spherical shape nanoparticles provide the worst outcome. Roy [42] studied the heat transfer characteristic between a square enclosure and a circular, an elliptical, or a rectangular cylinder. The numerical investigation stated that the Nusselt number linearly increased at the inner and outer cylinder for the high value of the volume fraction of nanoparticles while the Rayleigh number increased exponentially. In a square enclosure comprising a solid cylinder, Jami *et al.* [43] discovered impressive findings on natural convection flow. In a square chamber with a square block for low Prandtl number fluid, Sheikhzadeh *et al.* [44] investigated the influence of duration ratio on magneto-convection. Meanwhile, Jani *et al.* [45] studied MHD

free convection in a square cavity. They discovered that, for low Rayleigh numbers, increasing the Hartmann number suppressed free convection, and heat transfer has primarily through conduction. Ali *et al.* [46] examined MHD free convection flow in a differentially heated square cavity with the tilted obstacle. They discovered that the effect of higher Rayleigh number and lower Hartmann number resulted in significant heat transfer enhancement, with the contrary phenomenon also observed in the case of average temperature.

The present research numerically investigated the natural convection of heat transfer and fluid flow of Fe_3O_4 -water nanofluid inside the trapeziform cavity for a large variation of Rayleigh numbers, Prandtl numbers and nanoparticle volumetric ratio. Here we consider the bottom wall is heated whereas the top wall is cold, and the left and right walls are kept as insulated. The results have been given in terms of streamlines, isothermal contours plots, and the temporal influence on average Nusselt number over a wide range of different investigated parameter values. All equations are solved numerically using the finite element method of the Galerkin weighted residual (GWR) technique.

1.5 Objectives

This research aims to simulate a two-dimensional convective-conductive heat transfer and laminar flow program using a trapezoidal enclosure. The specific aims of this research are as follows:

- To modify the mathematical model of heat and fluid flow applying nanofluid properties.
- To find heat transfer in a trapeziform cavity for ferrosferric oxide (Fe_3O_4)-water and Cu-water nanofluids.
- To visualize the laminar flows of a single nanofluid (Fe_3O_4 -water).
- To find the effects of various pertinent parameters like Rayleigh number, Nusselt number, and Prandtl number on flow and temperature fields.
- To compare the heat transfer performance of the mentioned single nanofluids using different solid volume fractions.

1.6 Possible Outcomes

Since the research proposal has been applied to nanofluid which is useful in nanotechnology,

industrial, and engineering applications, we may expect several important outcomes from it. These are summarized as follows:

- Variation of the different flow and heat-regulating parameters is expected to have a noticeable impact on the heat transfer and fluid flow structure inside the enclosure.
- The model may be used to discuss the effect of the effective viscosity of nanofluid on natural convection heat transfer in the trapeziform enclosure.
- It may be possible to identify the important impacts of exothermic chemical processes with Arrhenius kinetics on the streamline, resulting velocity, and temperature distribution.
- The results can be helpful in a wide range of applications including renewable energy, oil recovery, electronic cooling devices, solar collectors, cooling of nuclear reactors, petroleum industries, biological transportation and so on.

1.7 Scope of the Thesis

A brief description of the present numerical investigation of heat transfer inside a trapezoidal enclosure using nanofluids have been presented in this thesis through four chapters as stated below:

Chapter 1 contains introduction with the aim and objectives of the present work. This chapter also includes a literature review of the past studies on heat transfer using different types of fluids and nanofluids which are relevant to the present work. Objectives of the present study has also been included in this chapter.

Chapter 2 presents a detailed description for the numerical simulation of heat transfer and fluid flow characteristics inside a cavity taking heat transfer medium as water and water based single nanofluids. Mathematical formulation has been given for numerical computation in this chapter.

In Chapter 3, the effects of Rayleigh number, Prandtl number, Nusselt number and solid volume fraction of nanoparticle have been investigated. Results have been shown in isothermal lines, streamlines to better understand the heat transfer mechanism through trapeziform enclosure.

Chapter 4 concludes remarks of the whole research and the future research for the future research have been presented methodically.

2.1 Introduction

Numerical analysis, area of mathematics and computer science that creates, analyzes, and implements algorithms for obtaining numerical solutions to problems involving continuous variables. Such problems arise throughout the natural sciences, social sciences, engineering, medicine, and business. Since the mid-20th century, the growth in power and availability of digital computers has led to increasing use of realistic mathematical models in science and engineering, and numerical analysis of increasing sophistication is needed to solve these more detailed models of the world. The formal academic area of numerical analysis ranges from quite theoretical mathematical studies to computer science issues. With the increasing availability of computers, the new discipline of scientific computing, or computational science, emerged during the 1980s and 1990s. The discipline combines numerical analysis, symbolic mathematical computations, computer graphics, and other areas of computer science to make it easier to set up, solve, and interpret complicated mathematical models of the real world. Numerical analysis is concerned with all aspects of the numerical solution of a problem, from the theoretical development and understanding of numerical methods to their practical implementation as reliable and efficient computer programs. Most numerical analysts specialize in small subfields, but they share some common concerns, perspectives, and mathematical methods of analysis.

2.2 Finite Element Method

The description of the laws of physics for space- and time-dependent problems are usually expressed in terms of partial differential equations (PDEs). For most geometries and problems, these PDEs cannot be solved with analytical methods. Instead, an approximation of the equations can be constructed, typically based upon different types of discretizations. These discretization methods approximate the PDEs with numerical model equations, which can be solved using numerical methods. The solution to the numerical model equations is, in turn, an approximation of the real solution to the PDEs. The finite element method (FEM) is used to compute such approximations. The finite element method (FEM) is a numerical technique for solving problems which are described by partial differential equations or can be formulated as functional minimization and used to perform finite element analysis of any given physical

phenomenon. It is necessary to use mathematics to comprehensively understand and quantify any physical phenomena, such as structural or fluid behavior, thermal transport, wave propagation, and the growth of biological cells. A domain of interest is represented as an assembly of finite elements. Approximating functions in finite elements are determined in terms of nodal values of a physical field which is sought. A continuous physical problem is transformed into a discretized finite element problem with unknown nodal values. For a linear problem a system of linear algebraic equations should be solved. Values inside finite elements can be recovered using nodal values.

The FEM is to divide a solution region into finite elements. The finite element mesh is typically generated by a preprocessor program. The description of mesh consists of several arrays main of which are nodal coordinates and element connectivities. Interpolation functions are used to interpolate the field variables over the element. Often, polynomials are selected as interpolation functions. The degree of the polynomial depends on the number of nodes assigned to the element. The matrix equation for the finite element should be established which relates the nodal values of the unknown function to other parameters. For this task different approaches can be used; the most convenient are the variational approach and the Galerkin method. To find the global equation system for the whole solution region we must assemble all the element equations. In other words, we must combine local element equations for all elements used for discretization. Element connectivities are used for the assembly process. Before solution, boundary conditions (which are not accounted in element equations) should be imposed. The finite element global equation system is typically sparse, symmetric, and positive definite. Direct and iterative methods can be used for solutions. The nodal values of the sought function are produced because of the solution.

Several approaches can be used to transform the physical formulation of the problem to its finite element discrete analog. If the physical formulation of the problem is known as a differential equation, then the most popular method of its finite element formulation is the Galerkin method. If the physical problem can be formulated as minimization of a functional then variational formulation of the finite element equations is usually used.

2.3 Problem Formulation

2.3.1 Physical model

The schematic diagram of the studied configuration has been depicted in the Figure 2.1. It consists of a two-dimensional trapezoidal enclosure of height H . The bottom surface has been assigned to temperature T_h while the top surface of the enclosure has been cooled at a constant temperature T_c . Under all circumstance $T_h > T_c$ condition has been maintained. The inclined surface of the trapezoid cavity has been thermally insulated. The heat transfer medium has been taken as water-based nanofluids consisting equal solid volume fraction of each nanoparticle like (Fe_3O_4). It has been also assumed that both the fluid and nanoparticles are in thermal equilibrium and there is no slip between them. The nanofluid used in the analysis has been considered as laminar and incompressible. The gravitational acceleration acts to the vertical downward surface.

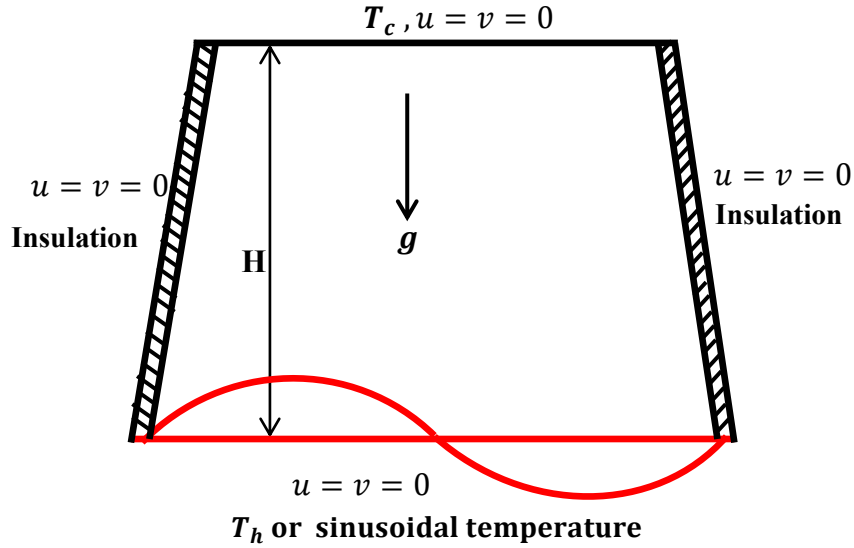


Figure 2.1: Physical model

2.3.2 Mathematical modeling

We assume a steady laminar flow of a viscous incompressible fluid having fixed properties. The well-known Boussinesq approximation is used to include buoyancy effect. Under the previous assumptions, the governing equation for momentum, mass and energy in a 2-D Cartesian coordinate system can be written as:

$$\frac{\partial u}{\partial x} + \frac{\partial v}{\partial y} = 0 \quad (1)$$

$$\rho_{nf} \left(u \frac{\partial u}{\partial x} + v \frac{\partial u}{\partial y} \right) = -\frac{\partial p}{\partial x} + \mu_{nf} \left(\frac{\partial^2 u}{\partial x^2} + \frac{\partial^2 u}{\partial y^2} \right) \quad (2)$$

$$\rho_{nf} \left(u \frac{\partial v}{\partial x} + v \frac{\partial v}{\partial y} \right) = - \frac{\partial p}{\partial y} + \mu_{nf} \left(\frac{\partial^2 v}{\partial x^2} + \frac{\partial^2 v}{\partial y^2} \right) + g(\rho\beta)_{nf} (T - T_c) \quad (3)$$

$$(\rho C_p)_{nf} \left(u \frac{\partial T}{\partial x} + v \frac{\partial T}{\partial y} \right) = k_{nf} \left(\frac{\partial^2 T}{\partial x^2} + \frac{\partial^2 T}{\partial y^2} \right) \quad (4)$$

Here u and v are the fluid velocity components in the x - and y - directions respectively, T - the temperature, p - the pressure, g - the gravitational acceleration, β –the coefficient of volumetric thermal expansion, ρ –the fluid density, ν –the kinematic viscosity, C_p –the specific heat at constant pressure and α –the thermal diffusivity.

The corresponding boundary conditions are:

$$\text{at left and right wall: } u = v = 0, \quad \frac{\partial T}{\partial n} = 0$$

$$\text{at bottom wall: } u = v = 0, \quad T = T_h \text{ (Uniform temperature)}$$

$$\text{or, } T = T_c + (T_h - T_c) \sin 2\pi x \text{ (Sinusoidal temperature)}$$

$$\text{at top wall: } u = v = 0, \quad T = T_c$$

where, n is the dimensional distances either along x or y direction acting normal to the left and right inclined surfaces.

The following dimensionless variables are used to non-dimensionalize the equations (1) - (4):

$$X = \frac{x}{H'}, \quad Y = \frac{y}{H}, \quad U = \frac{Lu}{\alpha_f}, \quad V = \frac{Lv}{\alpha_f}, \quad P = \frac{pL^2}{\alpha_f^2 \rho_f}, \quad \theta = \frac{T - T_c}{T_h - T_c} \quad (5)$$

Substituting the dimensionless variables in equations (1) - (4), one can obtain the following dimensionless form of the governing equations:

$$\frac{\partial U}{\partial X} + \frac{\partial V}{\partial Y} = 0 \quad (6)$$

$$U \frac{\partial U}{\partial X} + V \frac{\partial U}{\partial Y} = - \frac{\rho_f}{\rho_{nf}} \cdot \frac{\partial P}{\partial X} + \frac{\mu_{nf}}{\nu_f \rho_{nf}} Pr \left(\frac{\partial^2 U}{\partial X^2} + \frac{\partial^2 U}{\partial Y^2} \right) \quad (7)$$

$$U \frac{\partial U}{\partial X} + V \frac{\partial U}{\partial Y} = - \frac{\rho_f}{\rho_{nf}} \cdot \frac{\partial P}{\partial Y} + \frac{\mu_{nf}}{\nu_f \rho_{nf}} Pr \left(\frac{\partial^2 U}{\partial X^2} + \frac{\partial^2 U}{\partial Y^2} \right) + \frac{(\rho\beta)_{nf}}{\beta_f \rho_{nf}} Ra Pr \theta \quad (8)$$

$$U \frac{\partial \theta}{\partial X} + V \frac{\partial \theta}{\partial Y} = \frac{\alpha_{nf}}{\alpha_f} \left(\frac{\partial^2 \theta}{\partial X^2} + \frac{\partial^2 \theta}{\partial Y^2} \right) \quad (9)$$

where $Ra = \frac{g\beta(T_h - T_c)L^3}{\alpha_f \nu_f}$ and $Pr = \frac{\nu_f}{\alpha_f}$ are the Rayleigh number and Prandtl number. The

corresponding boundary conditions in a dimensionless form will become as follows:

all boundaries are rigid and non-slip, i.e., $U = V = 0$

at bottom wall: $\theta = 1$ (Uniform temperature)

or, $\theta = \sin(2\pi X)$ (Sinusoidal temperature)

at top wall: $\theta = 0$

at other walls: thermal insulation $\frac{\partial \theta}{\partial N} = 0$

The following models of effective properties of nanofluid have been chosen as:

$$\text{Thermal diffusivity, } \alpha_{nf} = k_{nf}/(\rho C_p)_{nf} \quad (10)$$

$$\text{Density, } \rho_{nf} = (1 - \phi)\rho_f + \phi\rho_s \quad (11)$$

$$\text{Heat capacitance, } (\rho C_p)_{nf} = (1 - \phi)(\rho C_p)_f + \phi(\rho C_p)_s \quad (12)$$

$$\text{coefficient of thermal expansion, } (\rho\beta)_{nf} = (1 - \phi)(\rho\beta)_f + \phi(\rho\beta)_s \quad (13)$$

$$\text{Specific heat at constant pressure, } C_{pnf} = \frac{(1-\phi)(\rho C_p)_f + \phi(\rho C_p)_s}{(1-\phi)\rho_f + \phi\rho_s} \quad (14)$$

$$\text{Viscosity of Brinkman model [47], } \mu_{nf} = \frac{\mu_f}{(1-\phi)^{2.5}} \quad (15)$$

Thermal conductivity of Maxwell-Garnett model [48],

$$k_{nf} = k_f \frac{k_s + 2k_f - 2\phi(k_f - k_s)}{k_s + 2k_f + \phi(k_f - k_s)} \quad (16)$$

The mean Nusselt number at the bottom surface of the enclosure:

$$Nu = -\frac{k_{nf}}{k_f} \frac{1}{L} \int_0^L \frac{\partial \theta}{\partial Y} dX \quad (17)$$

2.3.3 Thermo-physical properties

The thermophysical properties of nanofluids directly rely on the physical properties of material

and base fluids. These vary with the state variables temperature and pressure without altering their chemical identity. Therefore, thermophysical properties of base fluids and nanoparticles can be simply defined as the characteristics of the fluids system as well as the material properties. We use specific heat capacity, density, thermal conductivity, electric conductivity, volumetric thermal expansion coefficients of nanoparticles and base fluids, and the viscosity of the base fluids at room temperature for our current nanofluid research. In Table 2.1, these thermophysical attributes of nanofluids have been presented.

Table 2.1: Thermo-physical properties of the base fluid and the solid nanoparticle [49]

Items	C_p ($Jkg^{-1}K^{-1}$)	ρ (kgm^{-3})	K ($Wm^{-1}K^{-1}$)	μ ($kgm^{-1}s^{-1}$)	β (K^{-1})
H₂O	4179	997.1	0.613	0.001003	21×10^{-5}
Fe₃O₄	670	5180	80.4	-	20.6×10^{-5}
Cu	385	8933	401	-	1.67×10^{-5}

2.4 Numerical Analysis

To solve the governing dimensionless equation and the boundary conditions, the Galerkin weighted residual system of the finite element method has been used. In the process, the geometry is discretized into finite element meshes using non-uniform triangular elements. Six nodes triangular elements are used in this work for the development of the finite element equations. All six nodes are associated with the problem variables where pressure works on the corner nodes. A lower-order polynomial is chosen for pressure and satisfied through the continuity equation. In linear elements, the pressure is treated as discontinuous between the elements; otherwise, the whole domain has the same pressure. Applying Galerkin's weighted residual method Zienkiewicz and Taylor [50], the nonlinear governing partial differential equations are transferred into a system of integral equations. Gauss quadrature method or exact integration formula is used in each term to evaluate the integration. The nonlinear algebraic equations so obtained are modified by the imposition of variable thermal boundary conditions. To solve the set of the global nonlinear algebraic equations in the form of a matrix, the Newton-Raphson iteration technique has been adapted. Finally, a convergence criterion has been chosen

to obtain a numerical solution.

2.4.1 Grid Size sensitivity test

One of the essential steps before the problem's outcome generating is grid independence. Grid generation is a finite element technique for dividing a domain into a series of subdomains. At the discrete positions defined by the numerical grid, the variables are computed. It's essentially a discrete representation of the geometric domain that the issue must be addressed. One of the most essential aspects of the simulation is its independence from the number of grids used in the geometry. Table 2.2 and figures 2.2-2.3, show the average Nusselt number, Nu at the left vertical wall for various values of the triangular form of grids.

Table 2.2: The average Nusselt number at $Ra = 10000$, $Pr = 5.8$, $\phi = 0.01$ and constant temperature of bottom surface using water- Fe_3O_4 nanofluid

No. of elements	Nu	Time (s)
1184	6.04	28
1834	6.11	67
3062	6.15	99
8112	6.20	134
20129	6.204	342

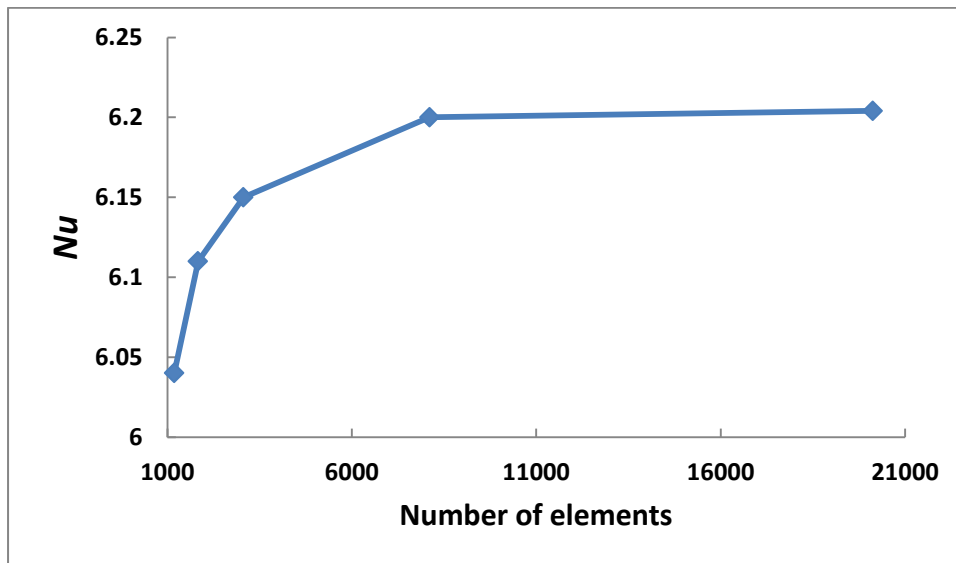


Figure 2.2: The average Nusselt number (Nu) for various number of elements

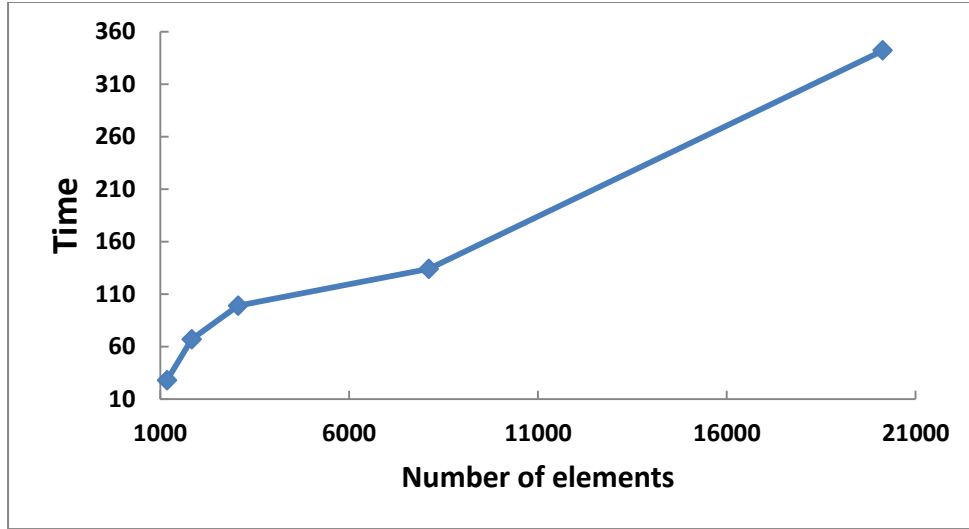


Figure 2.3: The processing time in second for various number of elements

The average Nusselt number has grown to a particular amount due to the growth in the number of elements in grid generation. After that, even if the elements grow larger, the value of the average Nusselt number remains almost unchanged as a result graph of the average Nusselt number is almost parallel to x -axis. The average Nusselt number grew by 2.65 percent as the number of elements increased from 1184 to 8112 whereas the average Nusselt number increased by 0.0064 percent and the processing time increased by 155.22 percent (Figure 2.3) when the number of elements increased from 8112 (Finer mesh) to 20129 (Extra finer mesh). This is indicating that the findings are independent of the number of elements in the domain. It has been utilized the 8112 elements as a grid-independent outcome in this study, and the results are true across all domains.

2.4.2 Meshing

A mesh that covers the geometric domain on which the problem is to be solved specifies the discrete positions at which the variables are to be computed. It divides the solution domain into finite elements, which are sub-domains with a finite number of sub-domains. The method's use of a set of finite elements to create computational domains with irregular geometries makes it a useful tool for solving boundary value problems in a wide range of engineering areas. Figure 2.4 displays the finite element mesh of the current physical domain. This figure represents the meshing of the present physical model with triangular finite elements.

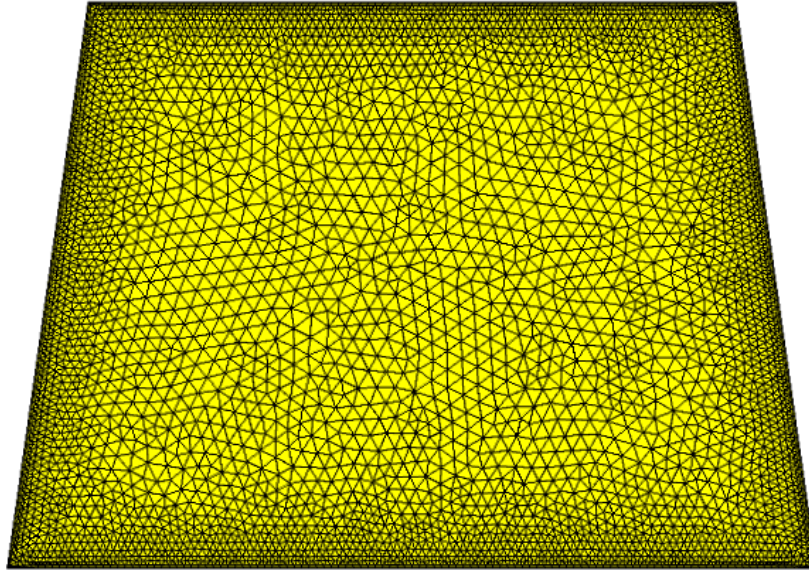


Figure 2.4: FEM mesh

2.4.3 Validation of the numerical scheme

Comparisons with previously published results are necessary to validate the correctness of the numerical results and the validity of the mathematical model developed during the current investigation. The results of the current numerical code are compared to those published by Basak *et al.* [51] for free convection flow in a square cavity uniformly heated from below whereas cooled from the other two vertical walls, and top wall is adiabatic. The streamlines and isotherms with $Pr = 0.7$ and $Ra = 10^3$ for the uniform temperature distribution at the bottom surface have been presented in the figure 2.5, that is a good agreement with Basak *et al.* [51]. The working fluid is water. As a result, the validation boosts the confidence in the numerical code to carry on with the above-stated objective of the current investigation.

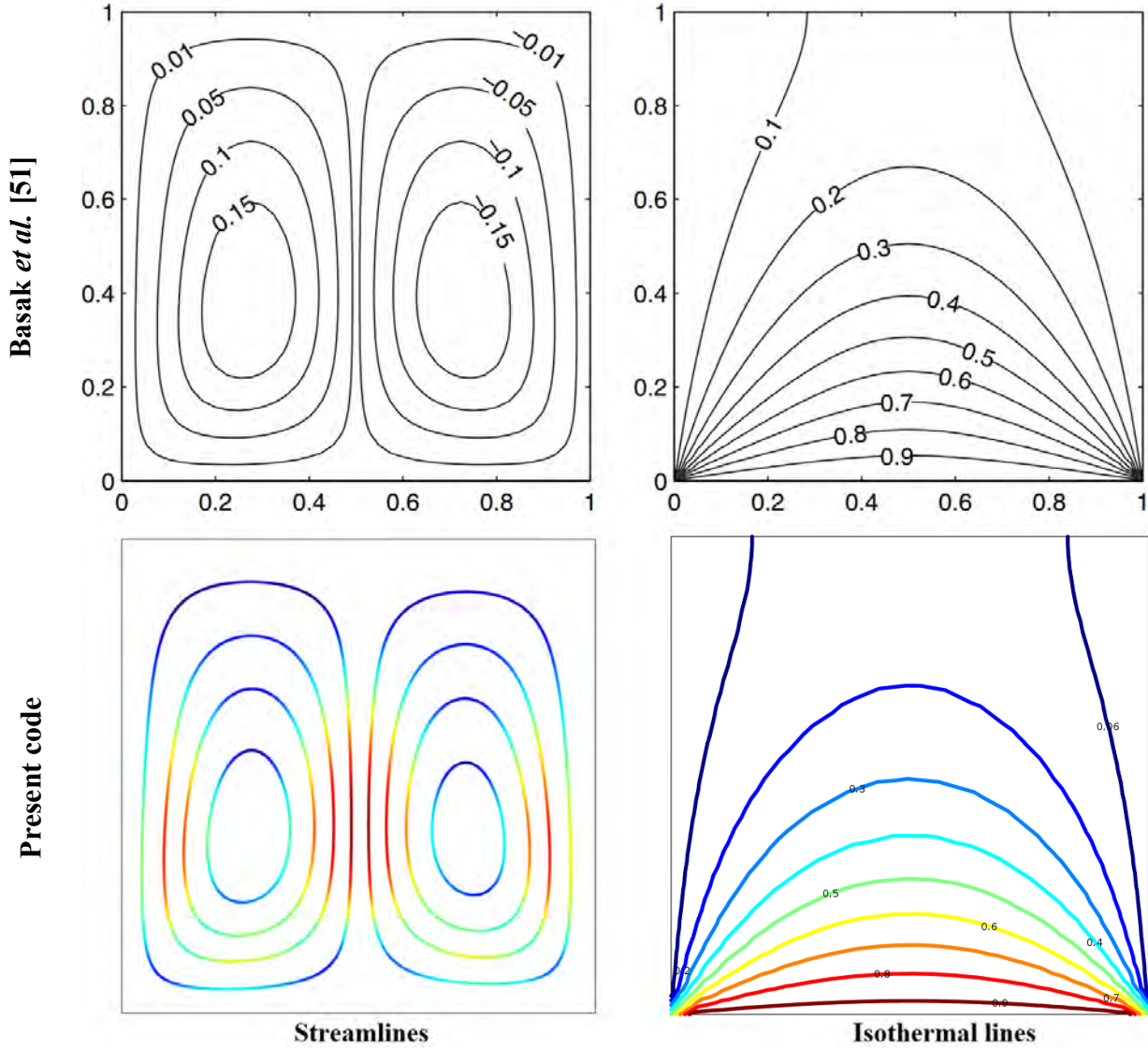


Figure 2.5: Code validation of present result with Basak *et al.* [51] at $Pr = 0.7$ and $Ra = 10^3$

3.1 Introduction

Natural convective heat transfer performance of water-based nanofluids (Fe_3O_4 -water) flow in a trapezoidal shaped enclosure has been investigated numerically. The numerical results of the current study are expatiated graphically via stream function contours (streamline), dimensionless temperature contours (isotherms) and local Nusselt numbers. The relevant parameters those have a direct effect on the flow and thermal fields inside the considered cavity are Rayleigh number, $Ra = 10^3 - 10^6$, Prandtl number, $Pr = 0.7$ to 5.8 and nanoparticles volume fraction, $\phi = 0$ to 3% . Also, shows Average Nusselt Number distribution along the bottom-side for the different values of Rayleigh number, Prandtl number and solid volume fraction. To display the results of these independent parameters, two parameters are fixed (unless where stated) while the remainder single one is varied as gathered in the following categories:

3.2 Effect of Rayleigh Number

Figure 3.1 represents the streamlines with constant heating and sinusoidal heating bottom side for four different thermal Rayleigh numbers $Ra = 10^3, 10^4, 10^5, 10^6$ with respect to the constant values of $Pr = 5.8$ and solid volume fraction $\phi = 1\%$ of water- Fe_3O_4 nanofluid. The significant change can be noticed in the pattern of streamlines for lower to higher Rayleigh numbers. For constant heating bottom wall two big vertical vortices are strongly visible for all Rayleigh numbers where the direction of the right vortex is anticlockwise, and the left vortex is clockwise which is due to the natural behavior of convection. For Rayleigh number 10^3 to 10^4 both the vortex is almost same size and for $Ra = 10^5$ the left vortex is larger than the right vortex. Besides this, a velocity layer is formed between the vortices for the all-Rayleigh numbers.

In addition, the velocity layer is practically perpendicular to the bottom wall, resulting in a larger buoyancy force. For higher Rayleigh numbers $10^3 \leq Ra \leq 10^6$, the core of the vortices tends to come in the amid of the cavity and elongate vertically to the colder wall. It is also observed that the density and the strength of the streamlines increased conspicuously due to the enhancement of the temperature difference within the entire trapeziform cavity. For higher buoyancy force ($Ra = 1 \times 10^6$) the size of the vortices is almost equal and covered most of the region of the cavity, which indicates the convection is superior. For sinusoidal temperature of bottom wall, a big vortex is visible for all Rayleigh numbers which is

clockwise and increasing the value of Rayleigh number the core of the vortex moves to left and the core of the vortex two tiny vortices are visible for $Ra = 10^6$.

Isotherm reflects the heat distribution inside geometry in a normal sense, and the influence of isotherm for four distinct Rayleigh numbers has reflected in the figure 3.2 with constant temperature (column- a) and sinusoidal temperature (column-b). The flow within the cavity is strongly generated by nanoparticles along with the rising values of the buoyancy-driven parameter, as seen in the picture. For lower thermal Rayleigh number $10^3 \leq Ra \leq 10^4$, heat lines are cluster adjacent to the hotter wall, which point out the conduction mode is active for this case. In the case of higher buoyancy force $10^5 \leq Ra \leq 10^6$, the density of the distorted thermal lines decreases and uniformly elongates to the colder wall due to the convection. Consequently, convection heat transfer is superior in the cavity for the higher Rayleigh number. Hence the heat transmission mode changed from conduction to convection as the thermal Rayleigh numbers increased.

The blue and red colours in the contour plot mean the lowest and highest value, respectively. The range of non-dimensional temperature values of isothermal lines are from 0 to 1 and from -1 to 1 for uniform and non-uniform temperature distribution at the bottom hot surface, respectively.

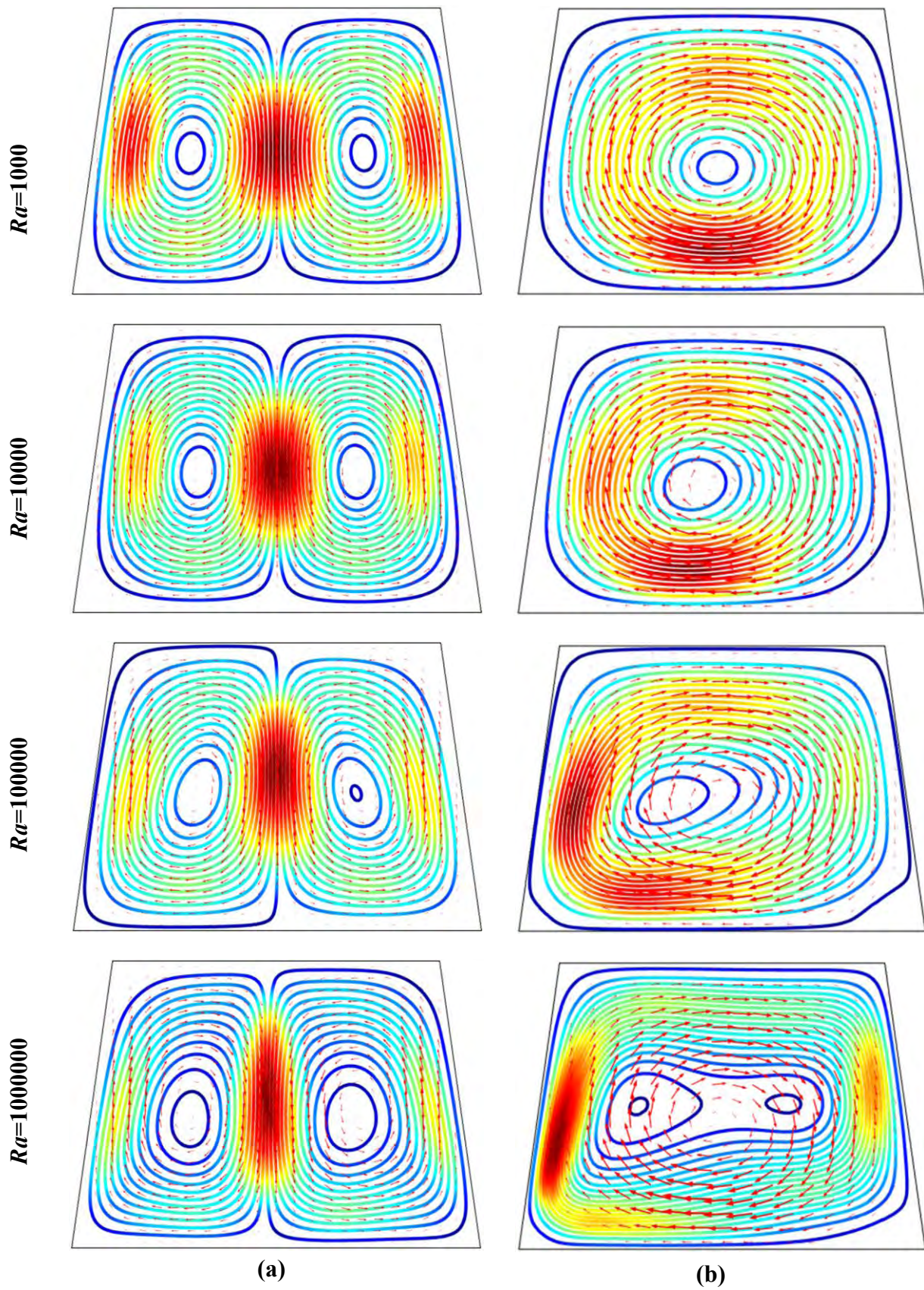


Figure 3.1: The streamlines for Rayleigh number variation with (a) constant temperature and (b) sinusoidal temperature at bottom wall

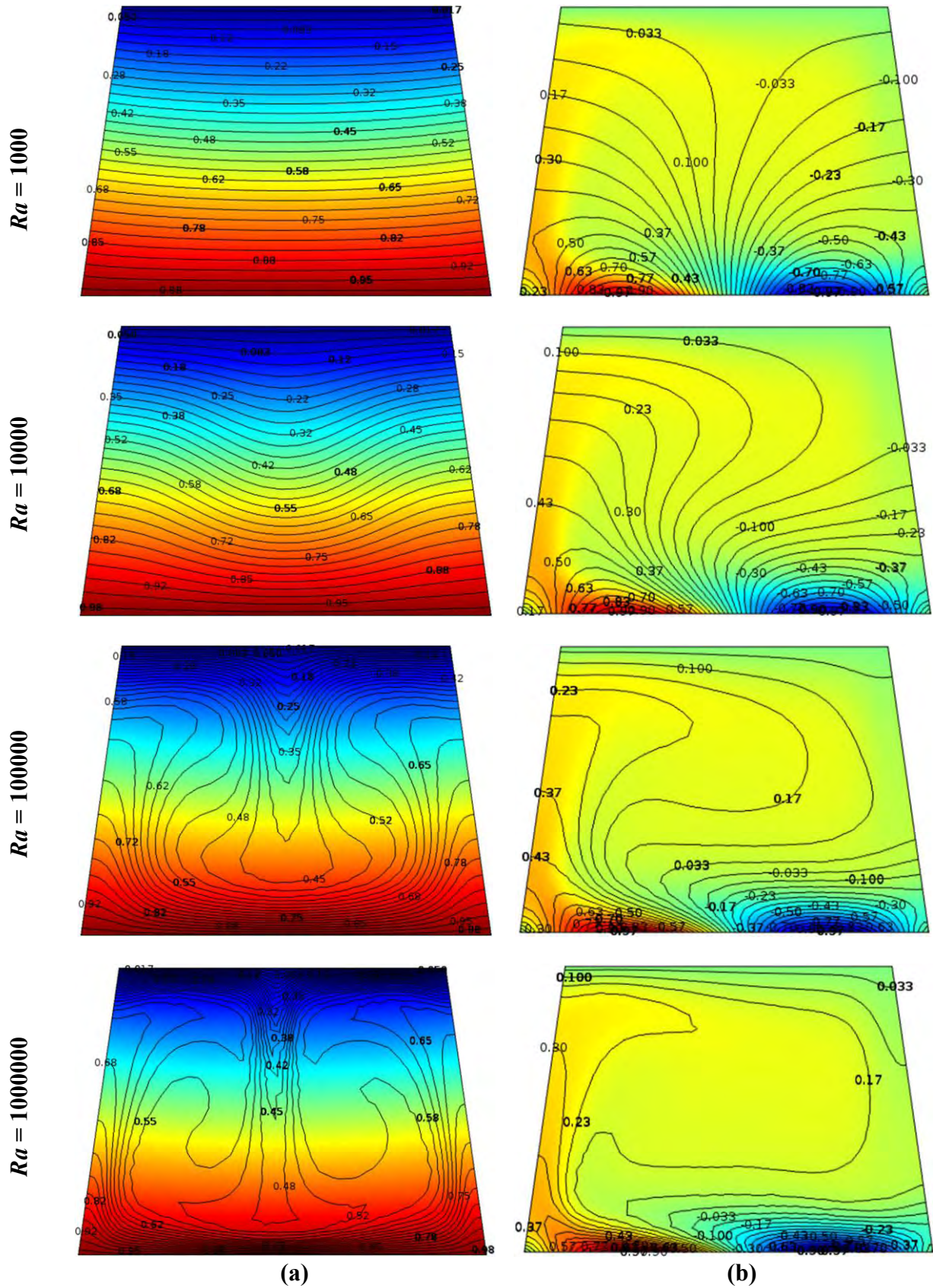


Figure 3.2: The isothermal lines for Rayleigh number variation with (a) constant temperature and (b) sinusoidal temperature at bottom wall

3.3 Effect of Prandtl Number

The consequences of the Prandtl numbers ($Pr = 0.7, 1, 3, 5.8$) has been shown in the figure 3.3 with respect to streamlines with constant temperature and sinusoidal temperature in terms of the constant parameters $\phi = 1\%$ of water- Fe_3O_4 nanofluid and $Ra = 10^4$. All the values of Prandtl number represent water at different temperatures. In this study, the water base nanofluid has been used, and examined the effects of Prandtl numbers 0.7, 1, 3, 5.8 at the temperatures of 25°C respectively. It's worth noting that Prandtl numbers and temperatures have an anti-proportional relationship. For constant temperature bottom wall, the two anti-directional spinning large vortices can be seen in the streamlines for all Prandtl numbers. The right vortex is spinning anti-clockwise, and the left vortex is spinning clockwise. Streamlines span the whole domain for all Prandtl numbers, although they tend to get crowded at higher levels. A velocity layer is apparent in the left big vortex with higher Prandtl numbers, and the right big vortex has a propensity to extend to the hotter wall. As the Prandtl number increases, the temperature of the base fluid decreases, but the viscosity of the base fluid increases which preventing the fluid from flowing freely. For sinusoidal temperature only one clockwise spinning vortex can be seen in the streamlines for all Prandtl numbers. Streamlines span the whole domain for all Prandtl numbers, and a tiny vortex is visible at right-bottom corner for Prandtl number $Pr = 1$.

It can also be noted that the core and pattern of the velocity lines are nearly constant for all investigated Prandtl numbers, which also indicate lower values of the resultant velocity of the fluid. Since the resultant velocity is lower for the effect of Prandtl numbers so it is obvious that the heat transfer will be also lower. The average heat transfer rate rose by 0.168 percent to 0.213 percent for the Prandtl number increased by 0.7 to 5.8, respectively, due to the conduction behavior of heat transfer. Figure 3.4 displays the changes of the isothermal lines for the variation of Prandtl number from 0.7 to 5.8.

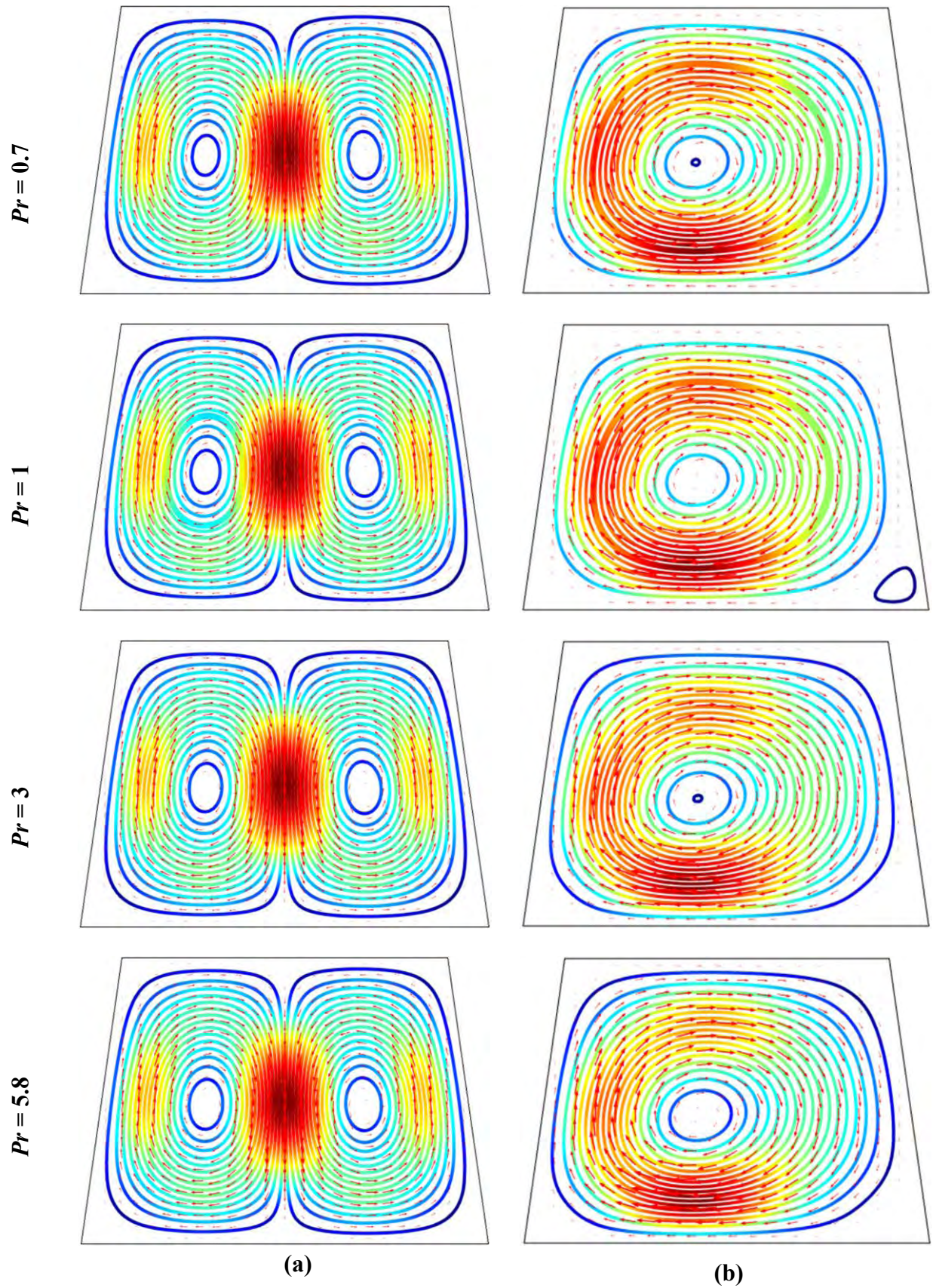


Figure 3.3: The streamlines for Prandtl number variation with (a) constant temperature and (b) sinusoidal temperature at bottom wall

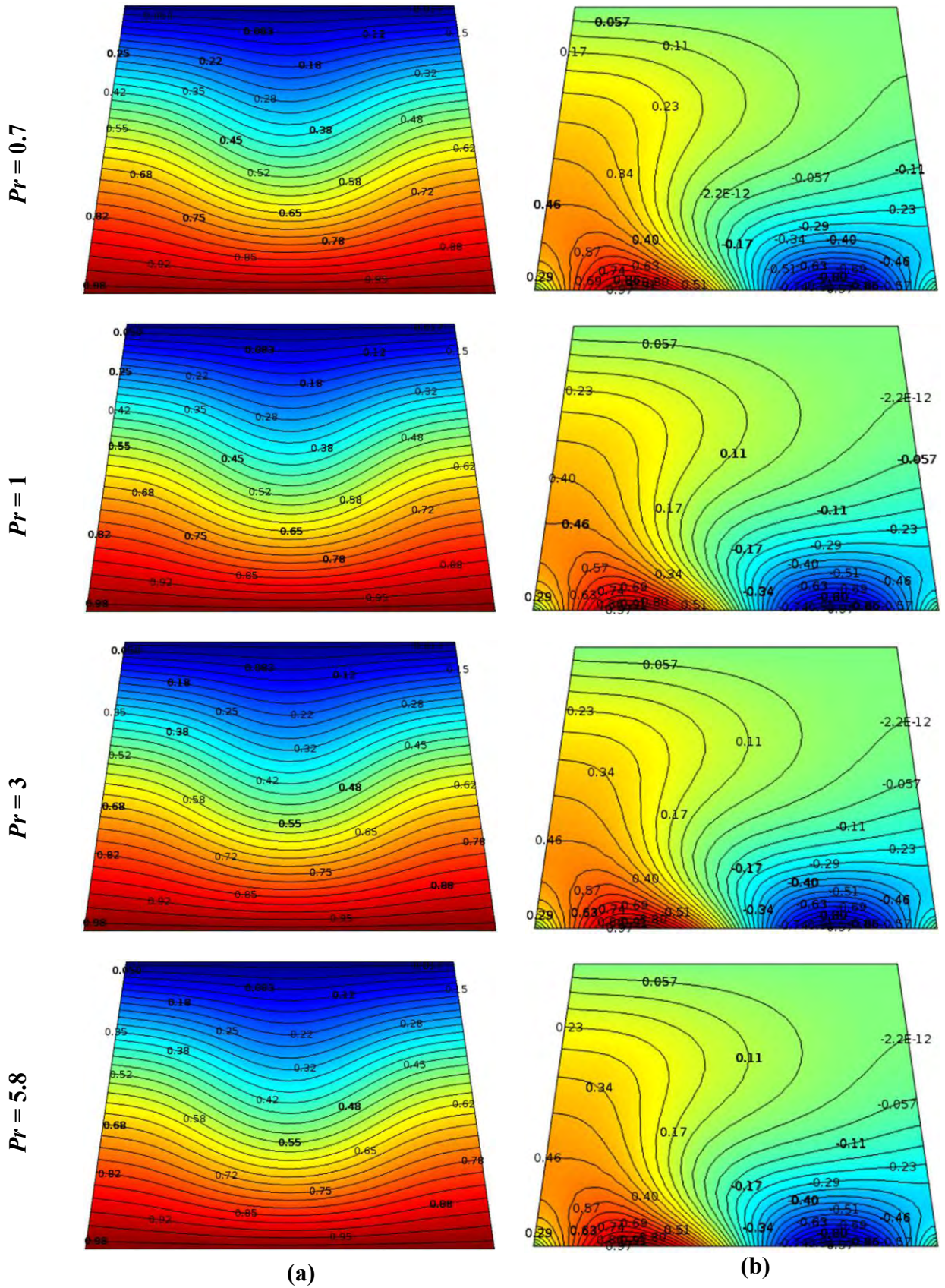


Figure 3.4: The isothermal lines for Prandtl number variation with (a) constant temperature and (b) sinusoidal temperature at bottom wall

3.4 Effect of Solid Volume Fraction

The effect of streamline for constant temperature bottom wall (column-a) and sinusoidal temperature bottom wall (column-b) are shown in the figure 3.5 and isothermal contour for constant temperature bottom wall (column-a) and sinusoidal temperature bottom wall (column-b) are shown in the figure 3.6 for the various volumetric ratios ($\phi = 0\%$, 1% , 2% , 3%) of ferrosopheric oxide nanoparticle with the fixed value of the parameters $Ra = 10^4$. For four distinct ratios of nanosolids, the spectacular impact of streamlines and isotherm has been seen for both cases.

Two large vortices are detected with anti-direction spinning for constant temperature and only one very big vortex is seen with clockwise direction for sinusoidal temperature for both the base fluid and the nanofluid. For constant temperature the direction of the streamlines of the right large vortex is counterclockwise, whereas the other vortex is clockwise. The velocity layer is remarked among the vortices. In the case of nanofluid, the velocity layer is more active in the vicinity of the wall. The core of the vortices tends to move to the center, indicating that the dominant fluid flows throughout the cavity, for a larger amount of nanoparticle volumetric ratio. The most noticeable difference between nanofluid and base fluid is that the streamlines become more clogged and tighter. This is owing to the presence of nanoparticles, which raised the density of the nanofluid and enhanced temperature differences due to collisions between nanoparticles.

Nanoparticles mixing with the base fluid play an important role in heat transfer, this phenomenon is shown in the last column of the figure 3.6. We have seen that the isotherms revolve with two counterclockwise and clockwise in the enclosure shows the dominant effects of the sinusoidal thermal wall conditions on the heat distribution. Without nanoparticles in the solution, the isotherms are loosely connected with contorted lines indicates the convection nature of the heat transfer. With the addition of nanoparticles with water, the density of the mixer increased and shows closely connected isotherm lines yield the significant heat transfer from species to species. For increasing the nanoparticle volumetric ratio ϕ from 0% to 3% , the average heat transfer rate increased by 5.83% for sinusoidal temperature and 7.38% for constant temperature distribution at the bottom surface of the trapeziform cavity. In conclusion, although the velocity of the fluid flow is decreased by the increase of nanoparticle volumetric ratio, but the average heat transfer rate increased.

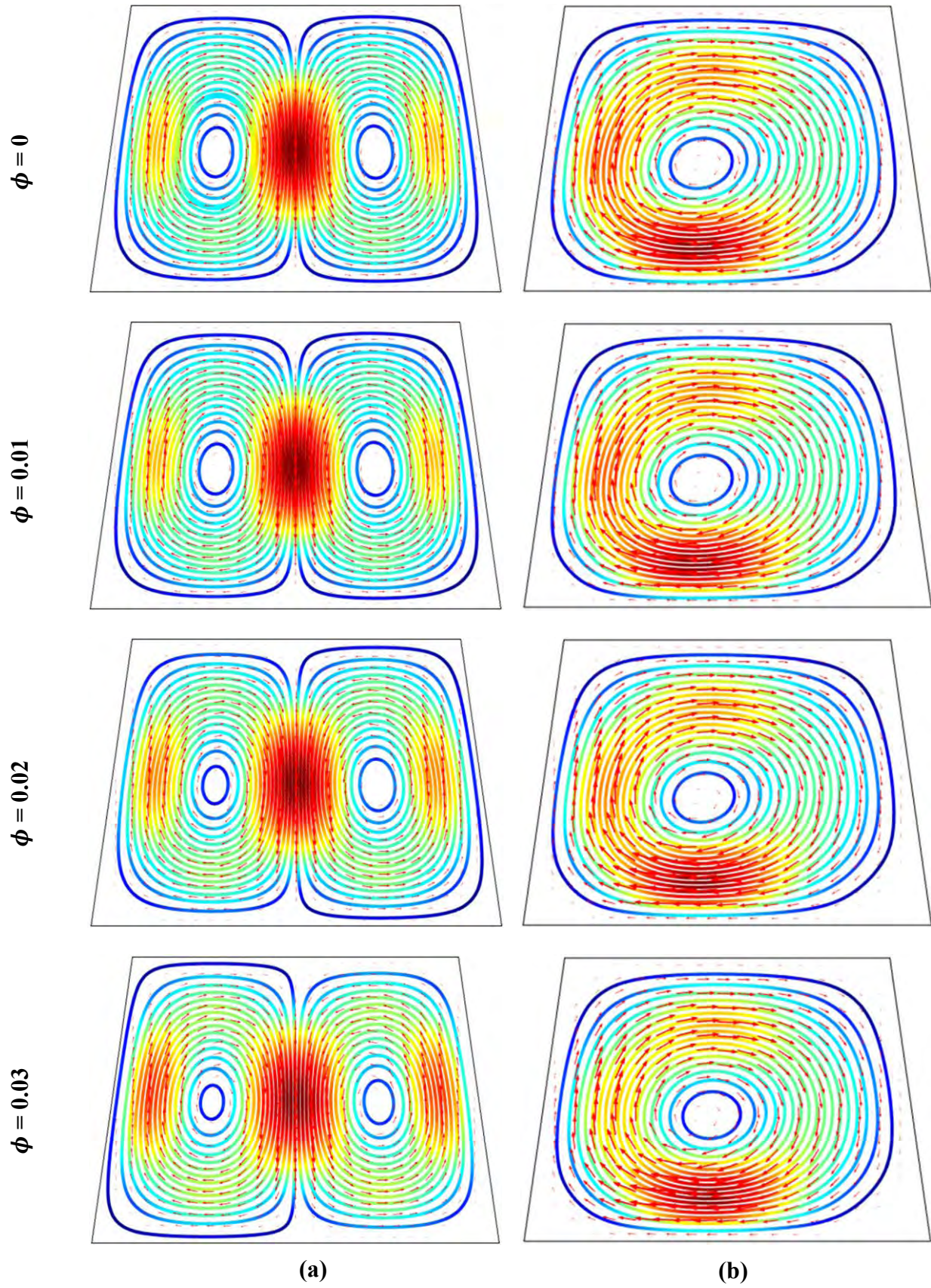


Figure 3.5: The streamlines for solid volume fraction variation with (a) constant temperature and (b) sinusoidal temperature at bottom wall

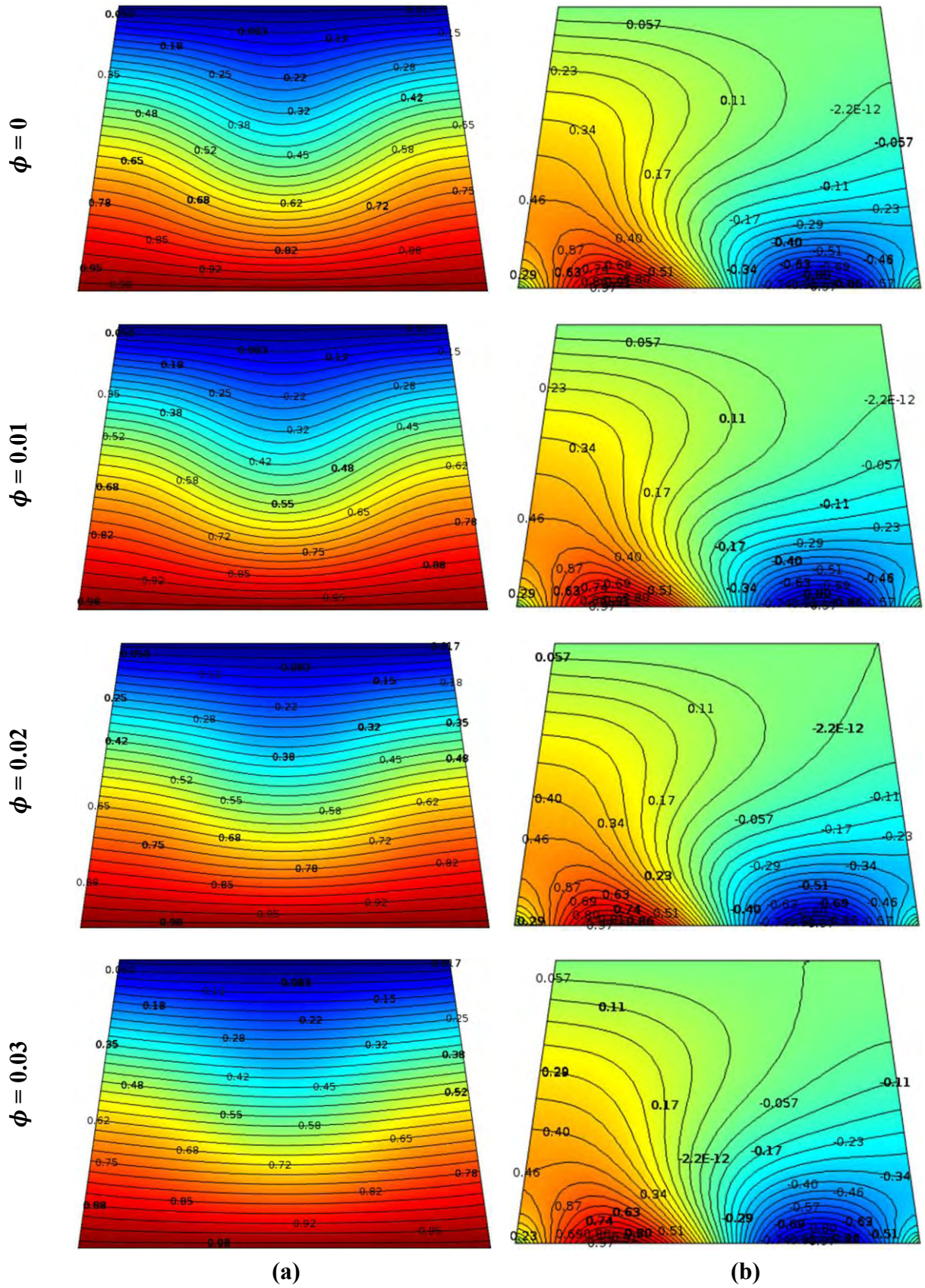


Figure 3.6: The isothermal lines for solid volume fraction variation with (a) constant temperature and (b) sinusoidal temperature at bottom wall

3.5 Nusselt Number

Figure 3.7 describes the effects of the mean Nusselt number for different values of Rayleigh numbers $Ra = 10^3, 10^4, 10^5, 10^6$ using $Pr = 5.8$ and solid volume fraction $\phi = 1\%$ of water- Fe_3O_4 nanofluid. At the beginning stage, the value of the average Nusselt number is 5.9 for sinusoidal temperature and 6 for constant temperature. The value of the average Nusselt number is increased for increasing the Rayleigh number. For the Rayleigh number 10^3 to 10^6 , the value of the average Nusselt number increases by 18.6% for sinusoidal temperature distribution of the heated bottom wall and 21.6% for constant temperature.

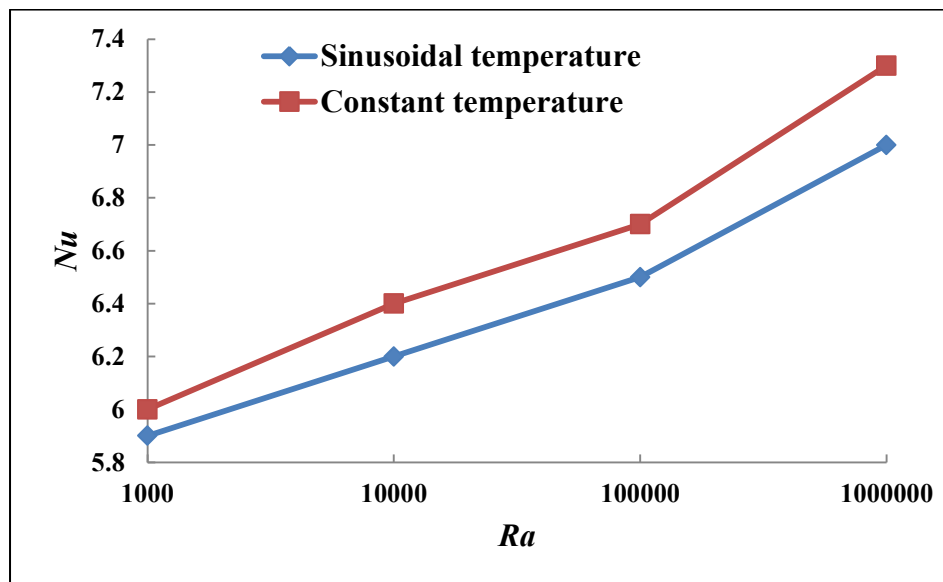


Figure 3.7: Mean Nusselt number for Rayleigh number variation

Figure 3.8 describes the effects of the mean Nusselt number for different values of Prandtl numbers ($Pr = 0.7, 1, 3, 5.8$) of $Ra = 10^4$ and solid volume fraction $\phi = 1\%$ of water- Fe_3O_4 nanofluid. At the initial stage, the value of the average Nusselt number is 5.5 for sinusoidal temperature and 5.6 for constant temperature. The value of the average Nusselt number is increased for increasing the Prandtl number. For the Prandtl number 1 to 5.8, the value of the average Nusselt number increases about 12.73% for sinusoidal temperature distribution and 14.28% for constant temperature of the heated bottom surface.

Figure 3.9 describes the effects of the mean Nusselt number for different values of the Fe_3O_4 and Cu nanoparticles volume fractions ($\phi = 0\%, 1\%, 2\%, 3\%$) with $Ra = 10^4$ and $Pr = 5.8$. At the first stage, the value of the average Nusselt number is 6 for sinusoidal temperature

distribution and 6.1 for constant temperature at the heated bottom surface. The value of the average Nusselt number is increased for increasing the nano-particle volume fractions. For the nanoparticle volume fractions 0 to 3%, the value of the average Nusselt number increases approximately 5.83% for sinusoidal temperature and 7.38% for constant temperature using water- Fe_3O_4 nanofluid and the value of the average Nusselt number increases approximately 12.63% for sinusoidal temperature and 15.57% for constant temperature using water-Cu nanofluid.

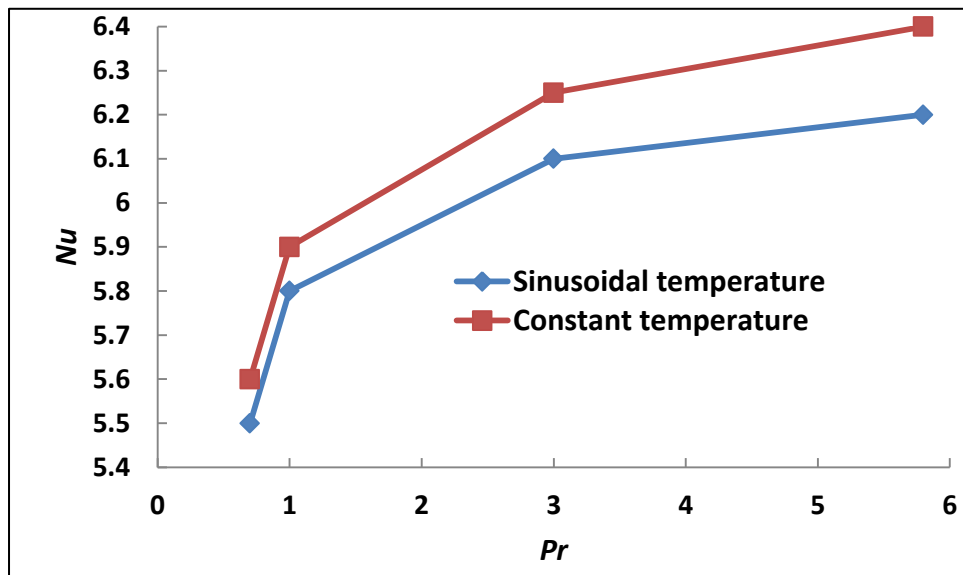


Figure 3.8: Mean Nusselt number for Prandtl number variation

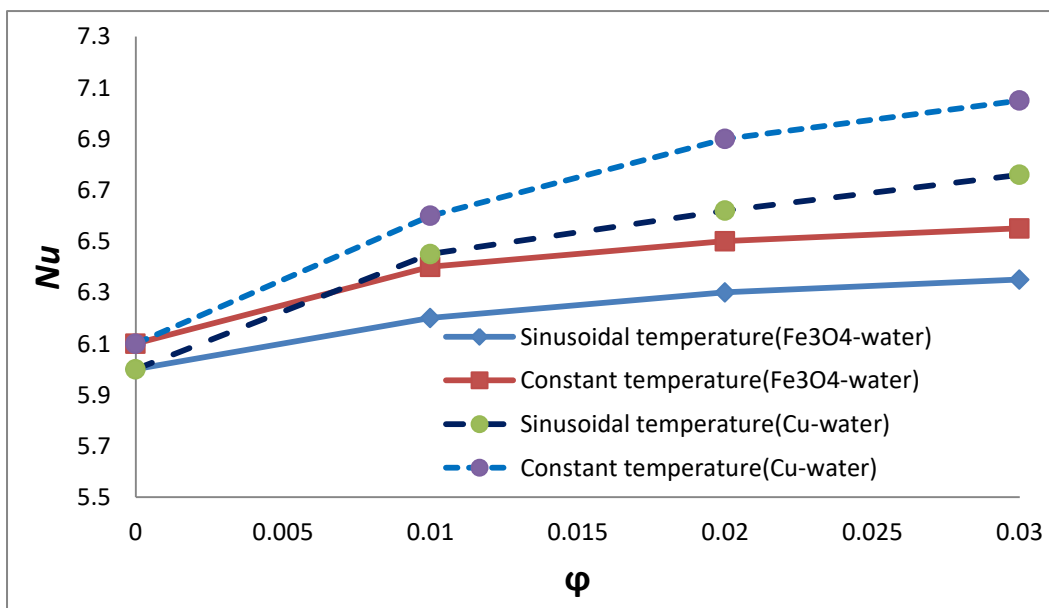


Figure 3.9: Mean Nusselt number for nanoparticle volume fraction variation for Fe_3O_4 -water and Cu-water

3.6 Comparison

3.6.1 Comparison with Basak *et al.* [51]

The comparison of the numerical results is a very imperative practice in computational dynamics. The numerical outcome of this study is supported by data from Basak *et al.* [51], who studied two-dimensional natural convection flow in a square cavity filled with water and present work has been studied two-dimensional natural heat convection flow in a trapezoidal cavity filled with water- Fe_3O_4 nanofluid. To make the comparison with the examined research work, the current code has been taken the parameter variation as same as Basak *et al.* [51]. The average Nusselt number is computed for base fluid water, $Pr = 0.7$ as fixed and variation of Rayleigh number from 10^3 to 10^5 . Figure 3.10 displays a graphical representation of the average Nusselt number in terms of Rayleigh number between Basak *et al.* [51] and the current study. It's important to note that the average Nusselt number is slightly higher for all values of Ra compared to Basak *et al.* [51].

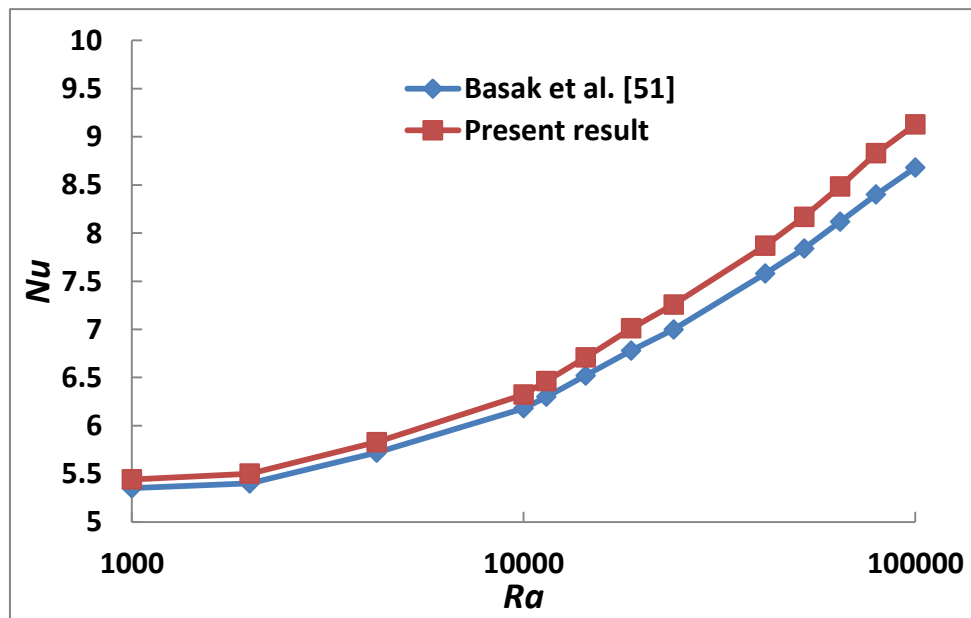


Figure 3.10: Comparison of average Nusselt number between Basak *et al.* [51] and present research

After all, it is strongly said that the current numerical code achieves excellent agreement with those of Basak *et al.* [51]. The numerical results from Basak *et al.* [51] and the current study work are also presented in table 3.1. The percentage of the inaccuracy of the values between these two studies is also included in this table. For Rayleigh number 10^3 , the minimal percentage of inaccuracy is 1.73 (approximately). The highest percentage of inaccuracy (about 5.17 percent) is caused by Rayleigh number 10^5 , for which the average Nusselt

number (Nu) derived from Basak *et al.* [51] and the current research is 8.68 and 9.13 respectively. In the comparison, a good agreement is discovered. The similarity of the comparisons encourages the current study's numerical results to be expanded.

Table 3.1: Comparison of average Nusselt number between present numerical study and the research of Basak *et al.* [51] in terms of Rayleigh number

Ra	Bashak <i>et al.</i> [51]	Present result	Percentage of error (%)
1000	5.35	5.44	1.73
10000	6.18	6.32	2.31
100000	8.68	9.13	5.17

3.6.2 Comparison with Weheibi *et al.* [52]

Weheibi *et al.* [52] studied two-dimensional natural convection heat transfer in a trapezoidal enclosure filled with water-Cu nanofluid. To make the comparison with the examined research work, the current code has been taken the parameter variation same as Weheibi *et al.* [52]. The average Nusselt number is computed for $\phi = 0.025$, $Pr = 0.7$ as fixed and variation of Rayleigh number from 10^3 to 10^6 . Figure 3.11 displays a graphical representation of the average Nusselt number in terms of Rayleigh number between Weheibi *et al.* [52] and the current study. It's important to note that the average Nusselt number is slightly lower for all values of Ra compared to Weheibi *et al.* [52].

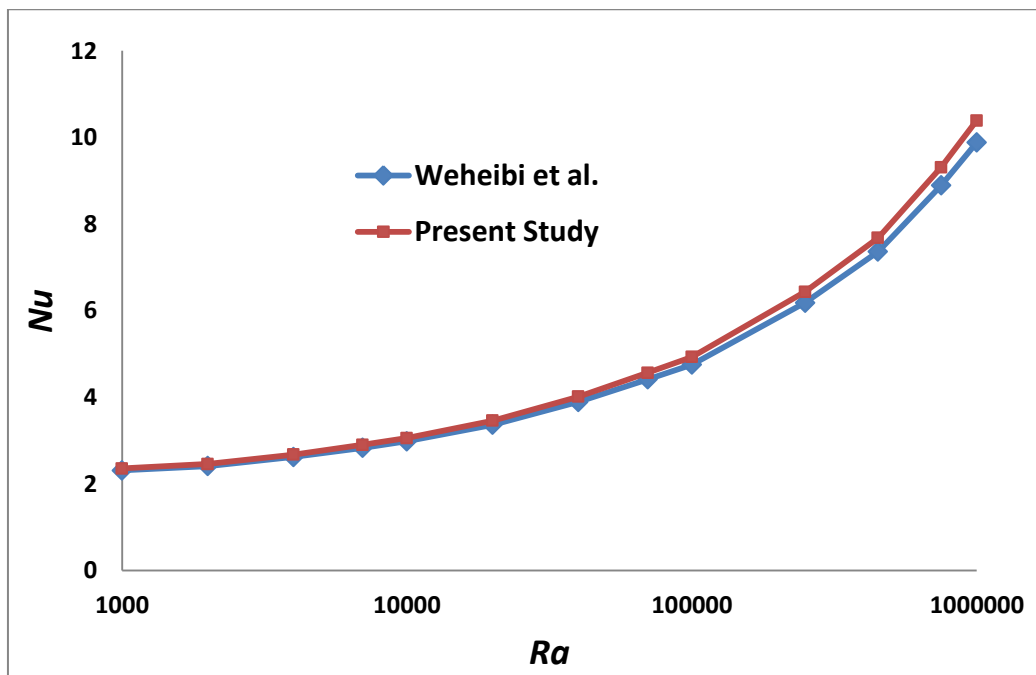


Figure 3.11: Comparison of average Nusselt number between Weheibi *et al.* [52] and present research.

The numerical results from Weheibi *et al.* [52] and the current study work are also presented in table 3.2. The percentage of the inaccuracy of the values between these two studies is also shown in this table. The minimal percentage of inaccuracy is 0.89 for $Ra = 10^3$ and the highest percentage of inaccuracy (about 4.13 percent) is for $Ra = 10^6$. The average Nusselt number (Nu) derived from Weheibi *et al.* [52] is 8.88 and the current research is 8.51 for $Ra = 10^6$.

Table 3.2: Comparison of average Nusselt number between present numerical study and the research of Weheibi *et al.* [52] in terms of Rayleigh number

Ra	Weheibi <i>et al.</i> [52]	Present result	Percentage of error (%)
1000	2.31	2.35	1.89
10000	2.98	3.05	2.51
100000	4.75	4.93	3.74
1000000	9.88	10.39	5.13

CONCLUSIONS AND FUTURE RESEARCH

4.1 Conclusions

The natural convective ferrosferric oxide (Fe_3O_4) water and copper (Cu) water nanofluids flow and heat transfer within the trapeziform enclosure using a dynamic model has been investigated numerically. The flow patterns, thermal fields of the nanofluid and base fluid, impacts of variables for different relatable parameters and effects of sloping angles of the cavity are investigated. The central results of the investigation can be summarized as:

- For the Rayleigh number 10^3 to 10^6 , the value of the average Nusselt number increases 18.6% for sinusoidal temperature and increases 21.6% for constant temperature. The value of the average Nusselt number using constant temperature becomes 16.13% higher than that of sinusoidal temperature distribution at the heated bottom surface.
- For the Prandtl number 0.7 to 5.8, the value of the average Nusselt number increases 12.73% for sinusoidal temperature and increases 14.28% for constant temperature. Higher value of Nu is found for constant temperature about 12.18% than that of sinusoidal temperature distribution at the bottom wall.
- Using Fe_3O_4 -water nanofluid increasing volume fraction upto 3%, mean Nusselt number increases 5.83% for sinusoidal temperature and 7.38% for constant temperature. Approximately 26.59% greater value of Nu is obtained using uniform temperature than sinusoidal temperature distribution at the bottom wall.
- Using Cu-water nanofluid, the average Nusselt number increases 13% for sinusoidal temperature and 15.57% for uniform temperature distribution due to the variation of solid volume fraction from 0% to 3%. The value of the mean Nusselt number for constant temperature is 19.8% higher than for sinusoidal temperature distribution at the bottom wall.
- Using Cu-water nanofluid higher rate of heat transfer 6.77% for sinusoidal temperature and 7.63% for constant temperature distribution at bottom wall are achieved using solid volume fraction $\phi = 0.03$ compared to water- Fe_3O_4 nanofluid.

4.2 Future Research

There is a lot of scope for research in this area in future. The size, shape, material, and volume fraction of dispersed nanoparticles play a very important role in the absorption of heat. In consideration of the present investigation, the following recommendation for future works have been provided:

- ◆ Trapezium shaped cavity has been considered in the present study. So, this deliberation may be extended by considering other formations of enclosures to investigate the performance of nanofluids.
- ◆ Using nanofluids with single phase flow have been considered as heat transfer medium in this work. It can be investigated for multiphase flow also.
- ◆ Natural convection heat transfer has been considered in the present study. This deliberation may be extended by considering force convection heat transfer.
- ◆ In this research, water-Fe₃O₄ nanofluid has been used as HTF. Anyone can use other combinations of nanofluids and hybrid nanofluids to obtain better heat transfer rate.

REFERENCES

- [1] M. Hasnaoui, E. Bilgen, and P. Vasseur, “Natural convection heat transfer in rectangular cavities partially heated from below”, *Journal of Thermophysics and Heat Transfer*, 6(2), (1992), pp. 255-266.
- [2] M.E. Arici, B. Sahin, “Natural convection heat transfer in a partially divided trapezoidal enclosure”, *Thermal Science*, 13(4), (2009), pp. 213-220.
- [3] K. Lasfer, M. Bouzaiane, T. Lili, “Numerical study of laminar natural convection in a side-heated trapezoidal cavity at various inclined heated sidewalls”, *Heat Transfer Eng.*, 31(5), (2010), pp. 362-373.
- [4] F. Selimefendigil, H.F. Öztop, A.J. Chamkha, “Analysis of mixed convection of nanofluid in a 3D lid- driven trapezoidal cavity with flexible side surfaces and inner cylinder”, *International Communications in Heat and Mass Transfer*, 87, (2017), pp. 40-51.
- [5] G.J. Weir, “The relative importance of convective and conductive effects in two-phase geothermal fields”, *Transport Porous Media*, 16(3), (1994), pp. 289-298.
- [6] D. Gao, Z. Chen, “Lattice Boltzmann simulation of natural convection dominated melting in a rectangular cavity filled with porous media”, *Int. J. Therm. Sci.*, 50(4) (2011), pp. 493-501.
- [7] J. Abdesslem, S. Khalifa, N. Abdelaziz, M. Abdallah, “Radiative properties effects on unsteady natural convection inside a saturated porous medium: Application for porous heat exchangers”, *Energy*, 61 (2013), pp. 224-233.
- [8] A.R.A. Khaled, K. Vafai, “The role of porous media in modeling flow and heat transfer in biological tissues”, *Int. J. Heat Mass Transfer*, 46(26), (2003), pp. 4989-5003.
- [9] M.M. Mousa, “Finite element investigation of stationary natural convection of light and heavy water in a vessel containing heated rods”, *Zeitschrift für Naturforschung A*, 67a (6/7), (2012), pp. 421-427.
- [10] M.E. Arici, B. Şahin, “Natural convection heat transfer in a partially divided trapezoidal enclosure”, *Thermal Science*, 13(4), (2009), pp. 213-220.
- [11] M.M. Rahman, H.F. Öztop, R. Saidur, S. Mekhilef, “Unsteady mixed convection in a porous media filled lid- driven cavity heated by a semi-circular heaters”, *Thermal Science*, 19(5), (2015), pp.1761-1768.

References

- [12] M.M. Mousa, "Modeling of laminar buoyancy convection in a square cavity containing an obstacle", *Bulletin of the Malaysian Mathematical Sciences Society*, 39(2), (2016), 483-498.
- [13] F. Selimefendigil, "Modeling and prediction of effects of time-periodic heating zone on mixed convection in a lid-driven cavity filled with fluid-saturated porous media", *Arab. J. Sci. Eng.*, 41(11), (2016), pp. 4701-4718.
- [14] F. Selimefendigil, M.A. Ismael, A.J. Chamkha, "Mixed convection in superposed nanofluid and porous layers in square enclosure with inner rotating cylinder", *International Journal of Mechanical Sciences*, 124-125, (2017), pp. 95-108.
- [15] M.A. Ismael, F. Selimefendigil, "Mixed convection in a vertically layered fluid-porous medium enclosure with two inner rotating cylinders", *Journal of Porous Media*, 20(6), (2017), pp. 491-511.
- [16] M.A. Sheremet, I. Pop, "Free convection in wavy porous enclosures with non-uniform temperature boundary conditions filled with a nanofluid: Buongiorno's mathematical mode", *Thermal Science*, 21(3), (2017), pp. 1183-1193.
- [17] A.M. Aramayo, S. Esteban, L. Cardón, "Conjugate heat transfer in a two stage trapezoidal cavity stack", *Lat.Am. Appl.Res.*, 39(1), (2009), pp. 1-9.
- [18] E. Papanicolaou, V. Belessiotis, "Double-diffusive natural convection in an asymmetric trapezoidal enclosure: unsteady behavior in the laminar and the turbulent-flow regime", *Int. J. Heat Mass Transfer*, 48(1), (2005), pp. 191-209.
- [19] K.S. Reddy, K.R. Kumar, "Estimation of convective and radiative heat losses from an inverted trapezoidal cavity receiver of solar linear Fresnel reflector system", *Int. J. Therm. Sci.*, 80, (2014), pp. 48-57.
- [20] M. Mahmoodi, "Numerical simulation of free convection of a nanofluid in L-shaped cavities", *International Journal of Thermal Sciences*, 50, (2011), pp. 1731-1740.
- [21] S. Soleimani, M. Sheikholeslami, D.D. Ganji, M. Gorji-Bandpay, "Natural convection heat transfer in a nanofluid filled semi-annulus enclosure", *Int. Commun. Heat Mass Transf.*, 39(4), (2012), pp. 565-574.
- [22] R. Roslan, H. Saleh, I. Hashim, "Buoyancy-driven heat transfer in nanofluid-filled trapezoidal enclosure with variable thermal conductivity and viscosity", *Numer. Heat Tran. Part A Appl.*, 60(10), (2011), pp. 867-882.

References

- [23] A. Shenoy, M. Sheremet, I. Pop, “Convective Flow and Heat Transfer from Wavy Surfaces: viscous fluids, porous media, and nanofluids”, *Chemical Rubber Company Press*, 2016.
- [24] S.A.M. Mehryan, E. Izadpanahi, M. Ghalambaz, A.J. Chamkha, “Mixed convection flow caused by an oscillating cylinder in a square cavity filled with cu–al₂o₃/water hybrid nanofluid”, *Journal of Thermal Analysis and Calorimetry*, 137, (2019), pp. 1–18.
- [25] O. Mahian, L. Kolsi, M. Amani, P. Estellé, G. Ahmadi, C. Kleinstreuer, and I. Pop, “Recent advances in modeling and simulation of nanofluid flows - Part I: Fundamentals and theory”, *Physics Reports*, 790, (2019), pp. 1-48.
- [26] A. Aghaei, H. Khorasanizadeh, G. Sheikhzadeh, M. Abbaszadeh, “Numerical study of magnetic field on mixed convection and entropy generation of nanofluid in a trapezoidal enclosure”, *J. Magn. Magn. Mater.*, 403, (2016), pp. 133–145.
- [27] H. Alipour, A. Karimipour, M.R. Safaei, D.T. Semiromi, O.A. Akbari, “Influence of T-semi attached rib on turbulent flow and heat transfer parameters of a silver-water nanofluid with different volume fractions in a three-dimensional trapezoidal microchannel”, *Phys. E Low Dimens. Syst. Nanostruct.* 88, (2017), pp. 60–76.
- [28] M. Lomascolo, G. Colangelo, M. Milanese, A. De Risi, “Review of heat transfer in nanofluids: conductive, convective and radiative experimental results”, *Renewable and Sustainable Energy Reviews*, 43, (2015), pp. 1182-1198.
- [29] Z. Haddad, H.F. Oztop, E. Abu-Nada, A. Mataoui, “A review on natural convective heat transfer of nanofluids”, *Renewable and Sustainable Energy Reviews*, 16, (2012), pp. 5363-5378.
- [30] A. Zaraki, M. Ghalambaz, A.J. Chamkha, M. Ghalambaz, D. De Rossi, “Theoretical analysis of natural convection boundary layer heat and mass transfer of nanofluids: effects of size, shape and type of nanoparticles, type of base fluid and working temperature”, *Advanced Powder Technology*, 26, (2015), pp. 935-946.
- [31] M.U. Sajid, H.M. Ali, “Recent advances in application of nanofluids in heat transfer devices: a critical review”, *Renewable and Sustainable Energy Reviews*, 103, (2019), pp. 556-592.
- [32] N.C. Roy, “Flow and heat transfer characteristics of a nanofluid between a square enclosure and a wavy wall obstacle”, *Physics of Fluids*, 31(8), (2019), 082005.

References

- [33] L.M. Al-Balushi, M.J. Uddin, M.M. Rahman, "Natural convective heat transfer in a square enclosure utilizing magnetic nanoparticles", *Propulsion and Power Research*, 8, (2019), pp. 194-209.
- [34] M.A. Mansour, and S.E. Ahmed, "A numerical study on natural convection in porous media-filled an inclined triangular enclosure with heat sources using nanofluid in the presence of heat generation effect", *Engineering Science and Technology: An International Journal*, 18, (2015), pp. 485-495.
- [35] A.A.A. Arani, M. Kazemi, "Analysis of fluid flow and heat transfer of nanofluid inside triangular enclosure equipped with rotational obstacle", *Journal of Mechanical Science and Technology*, 33, (2019), pp. 4917-4929.
- [36] M. Bouhalleb, H. Abbassi, "Numerical investigation of heat transfer by CuO–water nanofluid in rectangular enclosures", *Heat Transfer Engineering*, 37, (2016), pp. 13-23.
- [37] R. Nasrin, M.A. Alim, A.J. Chamkha, "Combined convection flow in triangular wavy chamber filled with water–CuO nanofluid: effect of viscosity models", *International Communications in Heat and Mass Transfer*, 39, (2012), pp. 1226-1236.
- [38] N. Makulati, A. Kasaeipoor, M.M. Rashidi, "Numerical study of natural convection of a water–alumina nanofluid in inclined C-shaped enclosures under the effect of magnetic field", *Advanced Powder Technology*, 27, (2016), pp. 661-672.
- [39] S. Soleimani, M. Sheikholeslami, D.D. Ganji, M. Gorji-Bandpay, "Natural convection heat transfer in a nanofluid filled semi-annulus enclosure", *International Communications in Heat and Mass Transfer*, 39, (2012), pp. 565-574.
- [40] N.C. Roy, "Natural convection in the annulus bounded by two wavy wall cylinders having a chemically reacting fluid", *International Journal of Heat and Mass Transfer*, 138, (2019), pp. 1082-1095.
- [41] F. Selimefendigil, H.F. Öztop, N. Abu-Hamdeh, "Mixed convection due to rotating cylinder in an internally heated and flexible walled cavity filled with SiO₂–water nanofluids: effect of nanoparticle shape", *International Communications in Heat and Mass Transfer*, 71, (2016), pp. 9-19.
- [42] N.C. Roy, "Natural convection of nanofluids in a square enclosure with different shapes of inner geometry", *Physics of Fluids*, 30, (2018), 113605.

References

- [43] M. Jami, A. Mezhhab, H. Naji, “Numerical study of natural convection in a square cavity containing a cylinder using the lattice Boltzmann method”, *International Journal for Computer Aided Engineering and Software*, 25, (2008), pp. 480-489.
- [44] G.A. Sheikhzadeh, A. Fattahi, M.A. Mehrabian, M. Pirmohammadi, “Effect of geometry on magneto-convection in a square enclosure filled with a low Prandtl number fluid”, *The Proceedings of the Institution of Mechanical Engineers, Part E: Journal of Process Mechanical Engineering*, 225, (2010), pp. 53-61.
- [45] S. Jani, M. Mahmoodi, M. Amini, “Magnetohydrodynamic free convection in a square cavity heated from below and cooled from other”, *World Academy of Science, Engineering and Technology*, 7, (2013), pp. 329-334.
- [46] M.M. Ali, M.A. Alim, M.A. Maleque, S.S. Ahmed, “Numerical simulation of MHD free convection flow in a differentially heated square enclosure with tilted obstacle”, *AIP Conference Proceedings*, 1851, (2017), pp. 1-8.
- [47] H.C. Brinkman, “The viscosity of concentrated suspensions and solution”, *Journal of Chemical Physics*, 20, (1952), pp. 571-581.
- [48] J.C.M. Garnett, “Colours in metal glasses and in metallic films”, *Royal Society*, 203, (1904), pp. 385-420.
- [49] A. Gul, I. Khan, S. Shafie, A. Khalid, and A. Khan, “Heat transfer in MHD mixed convection flow of a ferrofluid along a vertical channel”, *PloS One*, 10(11), (2015) e0141213.
- [50] O.C. Zienkiewicz and R.L. Taylor, “The Finite Element Method”, *McGrow-Hill*, 2, (1989), pp. 16-48.
- [51] T. Basak, S. Roy, and A.R. Balakrishnan, “Effects of thermal boundary conditions on natural convection flows within a square cavity”, *International Journal of Heat and Mass Transfer*, 49, (2006), pp. 4525-4535.
- [52] S.M. Al-Weheibi, M.M. Rahman, M.S. Alam, K.Vajravelu, “Numerical simulation of natural convection heat transfer in a trapezoidal enclosure filled with nanoparticles”, *International Journal of Mechanical Sciences*, 131–132 (2017), pp. 599-612.